Instantaneous Hybridization Factor (IHF) Development for Hybrid Electric Vehicle Energy-Emissions Analyses Using Real-World, On-Board Data

November 2020

A Research Report from the National Center for Sustainable Transportation

Britt A. Holmén, The University of Vermont

Mitchell K. Robinson, The University of Vermont

National Center for Sustainable Transportation

THE UNIVERSITY OF VERMONT TRANSPORTATION RESEARCH CENTER

TECHNICAL REPORT DOCUMENTATION PAGE

1. Report No. NCST-UVM-RR-20-25	**2. Government Accession No.** N/A	**3. Recipient's Catalog No.** N/A
4. Title and Subtitle Instantaneous Hybridization Factor (IHF) Development for HEV Energy-Emissions Analyses Using Real-World, On-Board Data		**5. Report Date** November 22, 2020 **6. Performing Organization Code** N/A
7. Author(s) Britt A. Holmén, PhD, http://orcid.org/0000-0003-3020-4293 Mitchell K. Robinson, https://orcid.org/0000-0002-3709-638X		**8. Performing Organization Report No.** N/A
9. Performing Organization Name and Address University of Vermont Transportation Research Center Mansfield House 25 Colchester Avenue Burlington, VT 05405		**10. Work Unit No.** N/A **11. Contract or Grant No.** USDOT Grant 69A3551747114
12. Sponsoring Agency Name and Address U.S. Department of Transportation Office of the Assistant Secretary for Research and Technology 1200 New Jersey Avenue, SE, Washington, DC 20590		**13. Type of Report and Period Covered** Final Report (February 2019 – August 2020) **14. Sponsoring Agency Code** USDOT OST-R

15. Supplementary Notes
DOI: https://doi.org/10.7922/G2MW2FFT
Dataset DOI: https://doi.org/10.5061/dryad.2bvq83bnj
NCST project journal article: Robinson, M.K. and B.A. Holmén (2020) Hybrid-electric passenger car energy utilization and emissions: Relationships for real-world driving conditions that account for road grade. *Science of the Total Environment*, Volume 738, 10 October 2020, 139692. https://doi.org/10.1016/j.scitotenv.2020.139692

16. Abstract
Past research has shown on-road emissions patterns unique to HEVs, indicating the need to account for them in emissions models. The main objective of this work is to outline a framework for development of new HEV emissions models based on current knowledge of CV emissions. The premise is that accurate knowledge of the instantaneous (1 Hz) power split between the HEV combustion and electric propulsion sources can be used to modify existing CV emission models for HEV emission predictions that are currently lacking in regulatory models. The HEV power split metric, instantaneous hybridization factor (IHF), was developed and quantified with on-road data collected from a 2010 Toyota Camry HEV operating on a fixed route in hilly Vermont over all seasons. IHF is the second-by-second ratio of electric system power to total system power and accounts for energy storage in the high voltage battery. IHF ranges from -1 to +1 and varies widely with vehicle speed and VSP. Different road types on the driving route were associated with different proportions of binned IHF activity, which represent the three key HEV operating states defined in this study: electric-drive only (EDO), power recovery and electric-drive assist. A more detailed analysis of IHF relationships to tailpipe emissions and road grade is found in a recently published article (Ref 1).

17. Key Words Power split, HEV, emissions, PEMS, on-board diagnostics (OBD)	**18. Distribution Statement** No restrictions.		
19. Security Classif. (of this report) Unclassified	**20. Security Classif. (of this page)** Unclassified	**21. No. of Pages** 46	**22. Price** N/A

Form DOT F 1700.7 (8-72) Reproduction of completed page authorized

NCST

About the National Center for Sustainable Transportation

The National Center for Sustainable Transportation is a consortium of leading universities committed to advancing an environmentally sustainable transportation system through cutting-edge research, direct policy engagement, and education of our future leaders. Consortium members include: University of California, Davis; University of California, Riverside; University of Southern California; California State University, Long Beach; Georgia Institute of Technology; and University of Vermont. More information can be found at: ncst.ucdavis.edu.

Disclaimer

Acknowledgments

This study was funded, partially or entirely, by a grant from the National Center for Sustainable Transportation (NCST), supported by the U.S. Department of Transportation (USDOT) through the University Transportation Centers program. The authors would like to thank the NCST and the USDOT for their support of university-based research in transportation, and especially for the funding provided in support of this project. Original TOTEMS data collection was funded by the United States Department of Transportation through the University Transportation Center program at the University of Vermont Transportation Research Center (DTRT06-F-0018P). We also thank students in the Transportation Air Quality Laboratory at UVM, specifically Matthew B. Conger and Karen M. Sentoff, for their efforts in TOTEMS data collection and database development. The contents of this report reflect the views of the authors, who are responsible for the facts and accuracy of the information presented herein.

NCST

Instantaneous Hybridization Factor (IHF) Development for Hybrid Electric Vehicle Energy-Emissions Analyses Using Real-World, On-Board Data

A National Center for Sustainable Transportation Research Report

November 2020

Britt A. Holmén, Department of Civil and Environmental Engineering, University of Vermont

Mitchell K. Robinson, Transportation Research Center, University of Vermont

NCST

[page intentionally left blank]

TABLE OF CONTENTS

List of Tables

List of Figures

Instantaneous Hybridization Factor (IHF) Development for Hybrid Electric Vehicle Energy-Emissions Analyses Using Real-World, On-Board Data

EXECUTIVE SUMMARY

Given anticipated significant increases in the proportion of electric drive passenger vehicles (HEV, PHEV and full EVs) in the fleet to achieve a more sustainable transportation system, it is critical that we have reliable models of the hybrid (HEV and PHEV) tailpipe emissions behavior during real-world operation of these vehicles. This research addresses the need to model the operating and emissions behavior of HEV technology in response to real driving conditions (including high-resolution road grade). The University of Vermont Transportation Air Quality Laboratory (UVM TAQLab) previously collected a unique dataset of tailpipe emissions and on-board diagnostic (OBD) operating parameters using a custom on-board sampling system during on-road driving by one driver of a MY2010 Toyota Camry HEV over a fixed route through all seasons. Here, the HEV dataset was analyzed to develop a new metric to provide quantitative understanding of the relationships between hybrid system energy management and emissions. The new metric, instantaneous hybridization factor (IHF) was quantified at 1 Hz based on detailed analysis of the recorded OBD scantool data, combined with literature values for the Toyota 3rd Generation Hybrid Synergy Drive technology.

This report summarizes development of the IHF parameter and relationships between IHF and variables used in the vehicle specific power (VSP)-based emissions modeling framework of EPA's mobile source emissions model, MOVES. The results detail how OBD data collected from the hybrid system can be used together with insights on HEV planetary gearset constants from the literature to quantify the electric vs. combustion power split for a single HEV design. Only a subset of the measured OBD scantool parameters were used to compute IHF. The IHF calculation could be further simplified if it was possible to obtain faster and higher numerical resolution OBD data from HEVs for multiple controller area networks simultaneously. Specifically, the hybrid system's operating parameters (SOC, current and power flows to/from the motor/generators) and simultaneous measurements of conventional ICE operating parameters (RPM, torque, coolant and catalyst temperatures, O_2 sensor voltages, fuel injection, etc.) would enable confirmation of calculated parameters. The availability of faster and more comprehensive OBD data would also enable detailed analysis of the "restart" events of the HEV's ICE that are critically associated with high emission events throughout a driving trip.

The final project data associated with this work are available on Dryad as detailed in the Data Management section of this report. A recent peer-reviewed article, Robinson and Holmén (2020) [1], offers more detailed analysis and modeling of CO_2 and particle number (PN) tailpipe emission rates using IHF in a VSP-speed context.

Introduction

Study Motivation

There is still relatively little quantitative understanding of the emissions behavior of hybrid-electric vehicles (HEVs) despite the fact that past research documented on-road emissions patterns unique to HEVs that are associated with restart of the internal combustion engine (ICE), indicating the need to account for them in emissions models. For example, we previously documented ICE "**restarts**" produced elevated particle number (PN) emission events [2], [3], but we lack modeling tools to quantify these events based on HEV system variables. This information is critical for projections of emissions from the future motor vehicle fleet that is anticipated to have larger proportions of HEVs. Further, while laboratory studies of HEV emissions exist upon which inputs for models of mobile source emissions, such as EPA MOVES, could be based, these models currently do not support project-level (microscale) modeling of HEVs. Given that a significant increase in the proportion of electric drive vehicles (including HEVs, plug-in HEVs and full EVs) in the passenger and heavy-duty vehicle fleet is anticipated to achieve a more sustainable transportation system, it is critical that we have reliable models of HEV energy use and tailpipe emissions behavior during their real-world operation. This research addresses the need for an analysis framework that can be used to evaluate real-world HEV operation and associated emissions in response to real driving conditions (road grade, vehicle speed, ambient temperature). Given that HEV tailpipe emissions occur only when the ICE is on, new HEV emissions models could be based on current knowledge surrounding conventional vehicle (CV) emissions, if the instantaneous (1 Hz) power split between electric and ICE-propulsion can be quantified as a function of driving conditions.

Hybrid gasoline-electric passenger vehicles, both HEVs and plug-in HEVs (PHEVs), represent an "adoption bridge" to future (beyond 2030) widespread consumer acceptance and use of fully battery-electric vehicles due to the range anxiety issue of full EVs. The U.S. Department of Energy records showed Toyota capturing 69% of all 2019 HEV sales trends [4] and, in April 2019, Toyota offered their patents freely to encourage HEV sector growth [5]. Currently, the US sales of HEVs are around 2%, greatly surpassing PHEVs and EVs, but sales of all are generally increasing since the introduction of HEVs in 1999 ([6], Figure 1). A recent J P Morgan report on the 2025 vehicle fleet projected HEVs would comprise 25% of sales, globally. Given the recent economic downturn in response to the novel coronavirus (SARS- CoV-2) pandemic in Winter 2020, and past history of HEV sales (i.e., after 2008 "Great Recession; Figure 1), it remains to be seen when electrified vehicle sales will surpass their most recent 2013 peak. Regardless, CAFE standard and CO_2 emissions legislation pushing manufacturers to sell higher fuel economy vehicles (averaging 54.5 MPG by 2025), should increase HEV and PHEV sales in the US in the long term.

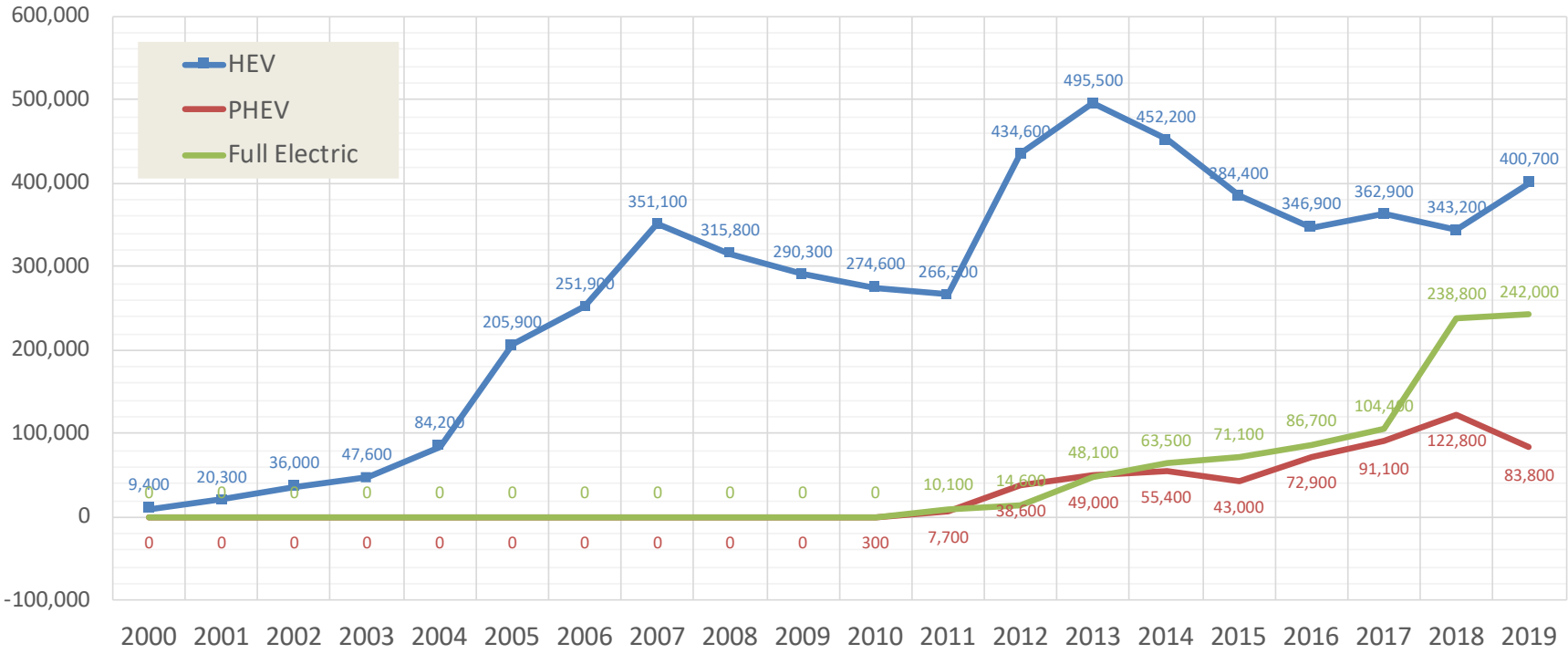

Figure 1. United States sales of light-duty electrified vehicles, 2000 – 2019 (Bureau of Transportation Statistics, 2020; Table 1-19)

This work focused on developing a new parameter that could serve as the basis for future HEV emissions models that are based on current knowledge of CV emissions behavior. It is well known that ICE emissions increase with engine load and transient operation, thus a load-based model that accounts for the proportion of propulsion power derived from the polluting combustion source is needed. Ignoring that HEVs generally have smaller displacement ICEs than the comparable model CV, the new metric developed here is based on the premise that accurate knowledge of the instantaneous (1 Hz) power split between the HEV's electrical and combustion propulsion sources as a function of driving parameters such as speed, grade and acceleration requirements can be used to modify existing CV emission models for HEV emission predictions that are currently lacking in regulatory models such as EPA's MOVES (Figure 2). Using data collected during on-road driving across all seasons in hilly Vermont terrain we account for the various HEV operating modes encountered during real-world driving. The new HEV power-split metric may be used to either modify the vehicle specific power (VSP) bin from which a CV emission rate would be selected, or directly adjust a measured CV emissions rate, in future HEV emissions models. By identifying a measurable set of OBD-II scantool parameters that would enable HEV emission estimates based on less intrusive measurements of real-world HEV activity, not costly full portable emissions measurement systems (PEMS) data, future models of HEV emissions could therefore be based on operations-specific CV emission rates measured under different driving conditions. We previously reported on CV/HEV CO_2 tailpipe emission ratios that ranged from 0.8 to 10 for the vehicles studied here in a VSP binning context, but the range varied with road type [7]. Thus, in future HEV emissions models, the power-split parameter must be employed to dynamically encompass (at least) an order of magnitude range in resulting HEV emission rates.

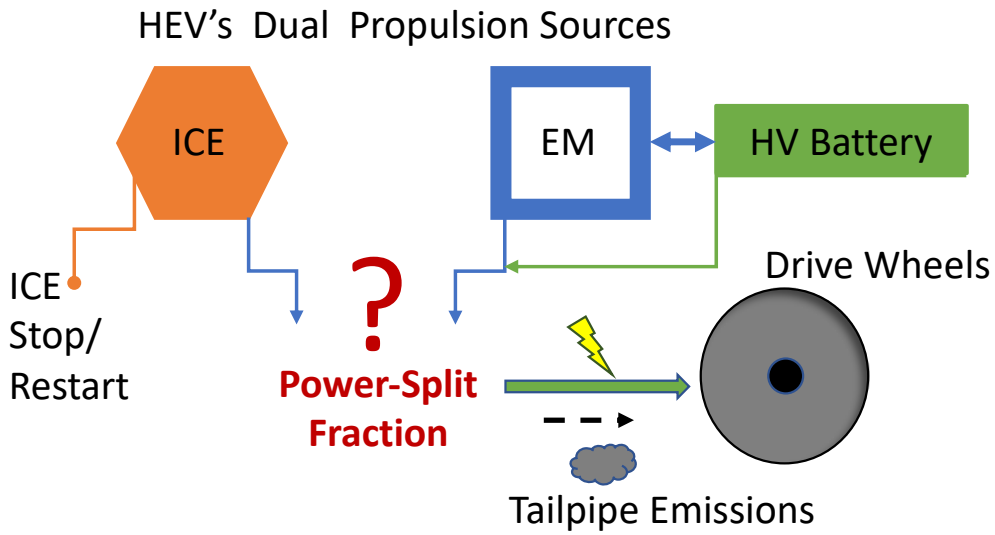

Figure 2. Schematic of HEV components and power-split fraction metric that quantifies, at each moment, the proportion of vehicle power derived from the conventional vehicle ICE powerplant or the HEV electric-drive system. Quantifying the 1 Hz power-split fraction based on real-world, on-board data is the focus of this work. ICE = internal combustion engine, EM = electric motor/generator, HV = high voltage.

Background on HEV Operation and Emissions

HEVs were designed to improve fuel economy. As less fuel is combusted, there are concomitant reductions in tailpipe emissions of both regulated pollutants – carbon monoxide (CO), hydrocarbons (HC), oxides of nitrogen (NOx = NO + NO_2) and particulate matter (PM) – and greenhouse gases (GHGs; carbon dioxide CO_2, methane CH_4, and nitrous oxide N_2O). Lower HEV fuel consumption and CO_2 emissions primarily accrue during city driving, with less HEV benefit for higher speed rural and freeway driving [7], [8]. Overall, relatively few studies have quantified emissions from light-duty HEVs; most prior studies examined fuel consumption, regulated pollutant and CO_2 emissions during simulated driving cycles on a chassis dynamometer [9]–[12] and one Toyota Prius study included the major greenhouse gases, CO_2, CH_4, and N_2O [13] . Tailpipe emissions from extremely low-emitting vehicles for dynamometer, real-world and test track driving included testing of 2003 Honda Civic hybrid-electric vehicles, but data reported were limited to averages of the criteria pollutants over all studied vehicles [14], [15].

A few light-duty HEV emissions studies have identified occasional high gas-phase and ultrafine particle emission events [2], [10], [16] that may be attributed to cooling of the catalytic converter during electric-only HEV operating modes. Early reports by Reyes (2006) suggested that steadily optimal catalysis temperature ranges may not be attainable for hybrid vehicles [13]. Because the typical three-way catalyst aftertreatment systems were designed for the more stable operating conditions produced by conventional vehicles (CVs), turning the ICE on and off in HEVs may cause catalyst inefficiencies, and result in intermittent relatively high emission events as documented for ICE “restarts” [2], [3], [10].

A more recent study reported fuel use, HC and CO emissions for three car pairs, each pair consisting of a CV and HEV of the same model type. On-road fuel use was 30% to 100% higher than laboratory results, but the HEVs still showed an on-road fuel benefit (the CVs used 23% to 49% more fuel than HEVs), and lower CO_2 emissions for the HEV compared to the same model CV [8]. However, HC and CO emissions were not lower for the HEVs, and only one CV/HEV vehicle pair showed lower NO for the HEV [8]. The authors attributed this to the ICE-restart behavior and diminished catalyst effectiveness. Duarte et al. (2014) indicated a similar observation and related emissions index to the duration of the ICE-off period. When the HEV ICE remained off for periods longer than 30 seconds, the CO and NOx emission index ratio increased 63% for CO and 73% for NOx [16]. Further, lower battery state of charge (SOC) was associated with increased fuel use and higher CO_2, CO and NOx emissions compared to mean operating results [16].

It is well documented that particulate matter has adverse effects on human health [17]–[19], with lung deposition increasing as particle size decreases [20] to fine (D_p < 2.5 µm), ultrafine (D_p < 100 nm) and nanoparticles (D_p < 50 nm). Currently, few on-road studies of hybrid passenger vehicle emission patterns exist, indicating a lack of understanding of the real-world effects of HEV emissions on air quality. Past laboratory work has indicated some similarities in emissions patterns between HEV and conventional vehicles (CV) [10]. For example, particle number emission rate (PNER) increased sharply for acceleration events, and was higher at higher vehicle

speeds compared to low vehicle speed for both HEV and CV [10]. However, HEV ICE restart events resulted in PNER several orders of magnitude higher than the studied CV and lasted several seconds in duration [10].

The HEV restart behavior has also been identified as a major source of particle number (PN) emissions under real-world driving conditions with higher PN emissions during urban [2], [3] and rural driving [3], compared to freeway driving where the CV was 2.4 times higher on average compared to the HEV [3]. These observations tie roadway driving characteristics to certain HEV operating modes that are sometimes distinct from CV operating modes. The largest CO_2 and fuel use benefit from HEVs were seen during city driving [7], yet this is where the highest HEV PN emissions occurred [2], [3]. This has implications on both emissions modeling, as HEVs make up larger portions of the total vehicle fleet, and human exposure in urban environments, suggesting increased hybridization of the vehicle fleet may not have the generally assumed benefit to urban air quality [2], [3], [8].

Hybridization Factor (HF)

Currently, emissions models do not distinguish between HEVs and CVs because they lack parameters to address HEV "power-split" metrics, or the proportion of total vehicle power generated that derives from the HEV electric motor/generator battery system. This report examines the HEV energy generation (capacity to do work) and power consumption (actual rate of doing work) at 1 Hz resolution for a 2010 Toyota Camry HEV, based on real-world, on-road driving scantool (OBD-II) measurements. We report on the development of a new parameter, the real-world, second-by-second, "*instantaneous* hybridization factor (IHF)". IHF is similar in concept, but to be distinguished from, the hybridization factor (HF; see Equation 1) used by hybrid vehicle *design engineers* when selecting HEV components.

Vehicle manufacturers define their power-split *design* specification, the hybridization factor (HF), as the ratio of the vehicle's maximum power from the electric motor(s) to the maximum power from both propulsion sources, electric motor (EM) and internal combustion engine (ICE) as shown in Equation 1 [21], [22]. By this definition, HF is a single value for any given vehicle design.

$$\mathbf{HF} = \frac{\mathbf{P_{EM,max}}}{\mathbf{P_{EM,max}} + \mathbf{P_{ICE,max}}} \qquad (1)$$

Where $P_{EM,max}$ is the electric motor's maximum power and $P_{ICE,max}$ is the ICE's maximum power (calculated from peak torque and RPM in the engine power curve). This HF design specification for HEVs *is of little use for emissions modeling because vehicles rarely operate at maximum power*. In this study, we hypothesize that defining a 1 Hz "instantaneous" HF (or "IHF"; see stylized Equation 7 below) during every second of driving – that quantifies the relative proportion of electric power being used at each moment – may provide a useful metric for future development of micro-scale emissions models for HEVs. This hypothesis reflects assumptions that when HEV ICE is off, there are zero emissions and that emissions increase with higher dependence on the ICE propulsion source to achieve requested vehicle power demand. Thus, we seek to define a parameter that quantifies HEV operations that are distinct

from CVs and therefore can possibly be used to "adjust" CV tailpipe emission rates (found in existing datasets) in order to model HEV emissions.

One prior 2001 Toyota Prius study developed an aggregated HEV emission model framework based on OBD scantool data on ICE speed (RPM) and vehicle speed, acceleration and vehicle specific power (VSP) thresholds that indicated when the HEV ICE was off/on, however, analysis was limited to average behavior in VSP bins and a limited range of VSP in dynamometer tests [23].

Vehicle Specific Power, Road Grade and Vehicle Emissions

Vehicle Specific Power (VSP) is the instantaneous vehicle power required to move the vehicle per unit vehicle mass [24]. There are four primary components to VSP: kinetic energy, potential energy, rolling resistance and aerodynamic drag (**Equation 2**). VSP is the current metric used in modal emissions models, such as EPA MOVES, to associate emission rates with vehicle operating modes; the MOVES model defines operating modes (OpModes) binned by VSP ranges within three vehicle speed categories [25].

$$VSP = \underbrace{1.1\text{va}}_{\text{Kinetic Energy}} + \underbrace{\text{vg} * \text{Gr}}_{\text{Potential Energy}} + \underbrace{\text{vg} * \text{Cr}}_{\text{Rolling Resistance}} + \underbrace{\frac{1}{2}\rho_a \frac{C_D A}{m} V^3}_{\text{Aerodynamic Drag}} \quad (2)$$

v = vehicle velocity (m/s)
a = vehicle acceleration (m/s^2)
g = gravitational constant (9.81 m/s^2)
Gr = road grade (%)
C_R = coefficient of rolling resistance = 0.0135 (dimensionless)
ρ_a = air density (kg/m^3): computed based on measured ambient temperature
C_D = coefficient of aerodynamic drag (dimensionless): CV = 0.28, HEV = 0.27
A = vehicle frontal area (m^2): manufacturer specification
m = vehicle mass (kg): total vehicle weight: CV = 1996 kg, HEV = 2136 kg

Road grade (Gr in Equation 2) is an important measure to enable quantifying the power use, and subsequent emissions, of on-road vehicles. Laboratory testing fails to capture this important metric, which has been shown to increase fuel use on hilly routes (average grade = 4%) when compared to flat by 15% to 20% [26]. Further, an increase in CO_2 emissions of 40% to 90% for grades ≥ 5% was seen compared with grades ≤ 0% [27]**.** Another study concluded that fuel use and emissions are underestimated by 16% to 22% if positive grades aren't accounted for, and overestimated by 22% to 24% when not factoring in negative grades [28]**.** In the on-board emissions dataset analyzed here, road grade field measurements were included in the dataset and used to compute VSP.

Readers are referred to the following journal paper for more detailed analysis of the on-road dataset with respect to the effects of road grade and road type (central business district, rural, suburban arterial, and freeway; as distinguished by speed limit) on HEV emissions:

> *Robinson, M.K. and B.A. Holmén (2020) Hybrid-electric passenger car energy utilization and emissions: Relationships for real-world driving conditions that account for road grade. Science of the Total Environment, Volume 738, 10 October 2020, 139692. https://doi.org/10.1016/j.scitotenv.2020.139692*

Methods

TOTEMS On-Board Emissions Dataset Description

On-board emissions and vehicle operating were previously collected by the research team using the Total Onboard Tailpipe Emissions Measurement System (TOTEMS:[29]**)** between February 2010 and September of 2011 along a fixed 51 km driving route in Chittenden County, Vermont. A total of 43 runs were collected on the 2010 Toyota Camry HEV and 32 runs on the 2010 Toyota Camry CV. Ambient temperature was between -10°C and +36°C across all runs. All TOTEMS data were collected at a 1-Hz rate. Vehicle electronic control unit (ECU) data were recorded using an OBD-II compliant scantool and Toyota Techstream software. For analysis, the full driving route was broken into 4 roadway classifications: Freeway (65 mph speed limit), Rural (45 mph speed limit), Suburban Arterial (40 mph speed limit) and Central Business District (CBD: 30 mph speed limit). Road grade along the route ranged from -13.2% to 11.5%, with a mean of -0.08%. Road grade was measured by the Vermont Agency of Transportation (VTrans) at 3-meter intervals to the nearest 0.1%. It was joined with the data based on recorded GPS locations using ESRI ArcGIS version 10.0. For the one-directional route employed for this study, freeway section grade (%) ranged from -6.4 to +4.3, and the rural, suburban arterial and CBD ranges were -13.2 to +11.5, -8.8 to +11.1, -6.6 to +10.8, respectively.

Tailpipe emissions were sampled with a specially designed tailpipe adapter that connected directly to the exhaust tailpipe and a 191°C heated transfer line. Second-by-second measurements included exhaust flowrate (pitot tube), exhaust temperature (thermocouples) and emission rates of total 5.6 to 562 nm particle number (TSI, Inc. Model 3090 Engine Exhaust Particle Sizer, EEPS) and 31 gases (MKS Multigas 2030-HS Fourier Transform Infrared Spectrometer (FTIR)). Fuel rate was calculated using the FTIR measurements of CO, CO_2 and C_3H_8 using the carbon balance method [7]**.** (See [30] for more detail on TOTEMS sampling methodology).

OBD-II Scantool Data for Toyota Camry HEV

One of the challenges with the TOTEMS sampling suite of instruments was finding a vehicle scantool that would reliably log the data from the HEV. Further, given that no prior studies had reported on HEV on-board diagnostic (OBD) parameters (and manufacturer trade secrets), Toyota's own scantool was selected. It, however, was limited in its ability to log data from multiple controller area networks (CANs) simultaneously. Therefore, the HEV parameters

shown in Table 1 were collected; the limited number (n=13) of parameters was restricted by the scantool's logging capabilities to maintain a 1Hz datastream.

Table 1. Toyota Techstream Scantool Raw Data for Hybrid-Electric Vehicle

Parameter	Description	Unit	Expected Minimum Value	Expected Maximum Value
Sample Time	Scantool Sample Collection Time	MM:SS.mmm		
Ambient Temperature	Ambient Temperature	°C	-30	40
Battery State of Charge	State of Charge (All Batteries)	%	40	85
Calculate Load	Calculated Load	%	0	100
Engine Coolant Temp	Engine Coolant Temperature	°C	0	120
Engine Spd	Engine Revolutions	rpm	0	5500
Generator(MG1) Rev	Generator Revolutions	rpm	-8000	12000
Generator(MG1) Torq	Generator Torque	Nm	-100	100
Motor(MG2) Revolution	Motor Revolutions	rpm	-600	8561
Motor(MG2) Torq	Motor Torque	Nm	-200	300
Regenerative Brake Torq	Regenerative Brake Torque	Nm	0	450
Vehicle Spd	Vehicle Speed	km/h	0	130
W_{IN} Control Power	Maximum Chargeable Power Out of HV Battery	W	-5000	-26000
W_{OUT} Control Power	Maximum Chargeable Power to HV Battery	W	20000	26000

Results

We first summarize the Toyota hybrid system based on a literature review. This background was necessary to development of IHF. It should be noted that for other HEV designs, a similar approach to that applied here could be used, but quantitative values of instrument constants will depend on manufacturer and design specifications. The common and relatively long history of the Toyota hybrid system design enabled access to prior work that quantified key HEV parameters in this study.

Dataset Description

The final dataset used for IHF development consisted of 156,082 total records of 1Hz OBD data for one MY 2010 Toyota Camry HEV from the TOTEMS full dataset. Due to equipment malfunctions, fewer records were available for examining the relationships to tailpipe emission rates of CO_2 and PN, but those results are reported in more detail in Robinson and Holmén (2020).

Toyota Hybrid System, 3rd Generation

The model year 2010 Toyota Camry HEV is powered by a 2.4 liter, Atkinson cycle ICE (147 hp @ 6000 rpm; 138 lb-ft @4400rpm; sequential multi-point fuel injection) and a manufacturer reported 105 kW electric motor rating, but past studies suggested it is actually 70 kW [31], [32]. We resolved the disparity by recognizing that the combined total maximum system power of the electric motor (MG2) and generator (MG1) is 105 kW [31]. The manufacturer reported fuel economy was 33 city/34 highway miles per gallon. The HEV Atkinson cycle ICE produces less power compared to an Otto cycle ICE (as in the comparable conventional Toyota Camry), but provides an overall increased fuel economy. The HEV's electric motor MG2 compensates for this ICE power deficiency.

Toyota's 3rd generation Hybrid Synergy Drive (HSD) is classified as a full (or planetary) hybrid system, meaning the vehicle can operate solely on battery power by utilizing electric motor MG2 for propulsion. Toyota's 3rd generation hybrid system uses a dual planetary gearset configuration with two electric motors (MG1 and MG2) that can operate both as motors and as generators. (See the Appendix for details on the dual planetary gear configuration and associated calculations.) Energy can be captured through regenerative braking by operating the electric motors as generators. The ICE is mechanically linked to MG1 on planetary gearset 1 (PG1) that controls the power split device (PSD). MG2 is connected to the ring gear on the second planetary gearset, intended for motor speed reduction, via a fixed carrier [33]. Thus, electric motor MG2 is the primary drive motor together with the ICE. Vehicle torque output and driveshaft RPM was calculated using Equations 3 and 4, respectively, based on published gearing ratios of the planetary gearsets [33] (See Appendix for details).

$$\mathbf{T_{out}(Nm)} = \mathbf{T_{ICE}}\left[\frac{\mathbf{K_1}}{\mathbf{1+K_1}}\right] + \mathbf{T_{MG2}} * \mathbf{K_2} \quad (3)$$

$$\mathbf{N_{out}(RPM)} = \mathbf{N_{ICE}}\left[\frac{\mathbf{1+K_1}}{\mathbf{K_1}}\right] - \frac{\mathbf{1}}{\mathbf{K_1}}\mathbf{N_{MG1}} \quad (4)$$

Where N is the rotation rate (RPM) and T is the torque (Nm) of the system component, K_1 is the ratio of the ring gear (78 teeth) and sun gear (30 teeth) for the planetary gear set 1 and K_2 is the corresponding ratio for the second planetary gear set. The fixed value of K_1 is 2.6 [32].

Using planetary gear configuration detailed in the Appendix, we determined that approximately 28% of the torque from the ICE is used to drive MG1, the remaining ~72% of the ICE's torque is sent to the power split device (PSD) and subsequently to drive the wheels (Figure 3). While the Toyota Techstream software scantool data collection limited the direct measurement of ICE torque, because of the mechanical link between the ICE and MG1, it was possible to calculate ICE torque directly from MG1 torque (Equation 5).

$$\mathbf{T_{ICE}(Nm)} = \frac{\mathbf{T_{MG1}}}{\mathbf{0.28}} \quad (5)$$

K_2 is calculated as the ratio of the ring gear (57 teeth) and sun gear (23 teeth) for the second planetary gear set that is used to increase the torque output of MG2 [32]. Therefore, K_2 = 2.478, meaning the torque increase is 2.478 times higher after the gearing from MG2.

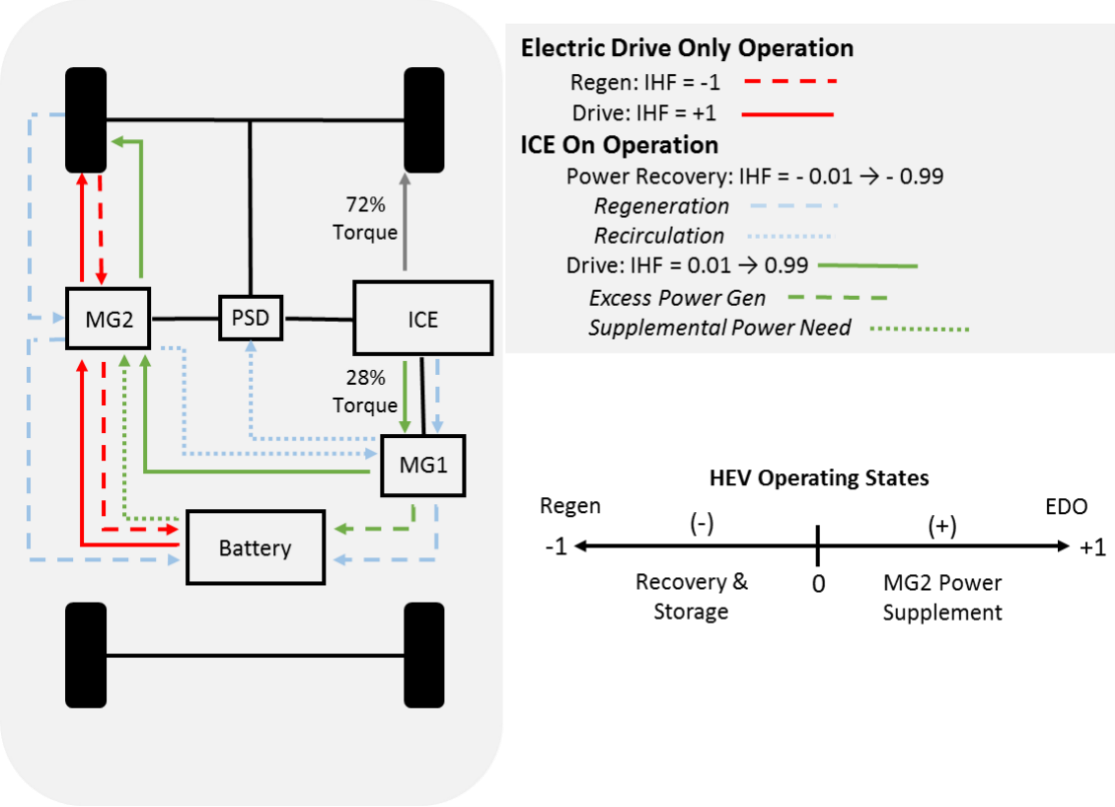

Figure 3. Toyota 3rd Generation Hybrid Synergy Drive (HSD) power flow directions (arrows between components) for different HEV operating states. Not shown is the inverter between the high voltage battery and the two electric motor/generators (MG1 and MG2). Corresponding ranges of IHF are shown in lower right.

Vehicle Power Output (VPO)

Similar to VSP, vehicle power output (VPO, Equation 6) could be defined as the instantaneous power used to move the vehicle based solely on actual vehicle ICE and MG2 torque and RPM measurements. VPO, in kilowatts, is a function of T_{out} and N_{out} (Equations 3 and 4) and constants to convert from radians/second to RPM and horsepower to kW. Like VSP, but calculated from the "input" side of motive power, VPO quantifies the power generated each second to meet the immediate propulsion needs. Both VSP and VPO do *not* account for any power generated or released from the HEV's high voltage battery, therefore they do **not** account for the total HEV's power.

$$\mathbf{VPO(kW)} = \mathbf{T_{out}(Nm)} * \boldsymbol{\omega}_{\mathbf{out}}\left(\frac{\mathbf{Rad}}{\mathbf{sec}}\right) = \frac{\mathbf{T_{out}} * \mathbf{N_{out}}}{\mathbf{7121}} * \mathbf{0.7457} \qquad \textit{(6)}$$

When considering the overall power management of an HEV that has two propulsion sources (ICE and electric system components), and the fact that tailpipe emissions may be dependent on the prior history of the vehicle's operation, IHF was developed to include accounting for battery storage, as described below.

Instantaneous Hybridization Factor (IHF)

Toyota's HSD system utilizes a complex energy management strategy to power the vehicle. To quantify the HEV power split for each second of driving, IHF was defined in general terms as *the ratio of electric system power to the total system power actually generated at each second of driving.* ***Equation 7*** *is a stylized equation intended to represent, using the absolute value symbols, what is a very complicated calculation because terms in Equation 7 drop out depending on the HEV's operating condition. In other words, the stylized Equation 7 must be used together with the conditions in Table 2 to arrive at the final quantitative value for IHF*. Utilizing the fact that MG1 and MG2 are generators when power is negative and motors when power is positive, the direction of power flow was determined. Further, keeping total system power positive allowed for the numerator in Equation 7 to control the sign of IHF.

$$\mathbf{IHF} = \frac{\textbf{Electric System Power}}{\textbf{Total System Power}} = \frac{\mathbf{P_{MG2}+P_{Battery}}}{[\mathbf{0.72*P_{ICE}}]+|\mathbf{P_{MG2}}|+|\mathbf{P_{Battery}}|} \quad (7)$$

Battery power ($P_{Battery}$) was quantified by the sign and direction of the instantaneous power generated by the two motor/generators, as $P_{Battery} = P_{MG2} + P_{MG1}$. Again, depending on the 1 Hz state of HEV operation, the final IHF calculation was performed using conditional statements to drop terms from Equation 7, as described in the next section and summarized in Table 2. These conditional statements, symbolized by absolute values on terms in the denominator of the general IHF expression in Equation 7, ensured there was no double counting of power flows. Absolute values were essentially needed to account for the *direction* of power flow. For example, when both MG2 and battery power were positive, the battery was supplying additional power to MG2. Therefore, in this case, battery power was accounted for in the IHF calculation as part of the MG2 power output, to avoid double-counting and the $P_{Battery}$ term would therefore not explicitly appear in the final IHF calculation expression.

Because the high-voltage battery only assisted the generator in powering the electric motor (MG2) when the generator (MG1) could not provide all the power being demanded, the total system power was reduced to the sum of ICE + electric motor power. In this case, the electric motor term, P_{MG2}, accounts for both $P_{Battery}$ and $P_{generator}$. For cases when the generator creates excess power not used immediately by the electric motor, total system power = ICE + electric motor + $P_{Battery}$. Thus, the absolute value controls for the sign conventions based on the way the data was recorded by the scantool. In another example, battery power that is negative during regenerative braking indicates power flow to the battery. In this case, using the conditional statements in the IHF calculation (see Table 2 below), battery power accounted for the regenerative braking power produced via MG2, so MG2 dropped out of the equation, Without the absolute value, this regenerative power would subtract from the ICE power (if the ICE was on), which would produce a negative value in the denominator and incorrectly assign a positive IHF during regenerative braking operation.

IHF can be negative due to the sign convention for MG2 and the battery: (+) values indicate power flows to the wheels and (-) sign indicates power flows to the battery for storage. We also defined IHF = 0 as the (rarely occurring) state where there is zero electric power assist. It should

be noted that total system power (Equation 7 denominator) fully accounts for the excess energy generation as well as storage within the HEV system that is critical for complete accounting and emissions modeling whereas, VPO and VSP do not.

Motor/Generator Sign and Power Flow Effects on IHF Calculation

IHF was defined to range from -1 (REGEN) to +1 (Electric-drive Only, EDO). The final IHF calculated value accounted for the HEV's different operating data states by applying IF/ELSE conditional statements based on the numerical order shown in Table 2. Recall that these conditions were used to account for the sign (+/-) of the electric motor power and battery power, calculated from the raw 1 Hz scantool measurements of MG1 and MG2 torque and RPM. Table 3 shows how the positive and negative IHF value ranges are interpreted in terms of the hybrid system's operation. The "conditions" column in Table 3 corresponds to the conditional statements defined in Table 2.

Table 2. Conditional Statements Used to Compute IHF*

Condition #	Description / Rationale	Resulting IHF Expression
1. RPM = 0 and vehicle speed = 0	It isn't possible for IHF = -1 if the vehicle is stationary (no regen braking) and the ICE is off (no MG1 power sent to the battery). So IHF must equal 1. This condition is required because if ICE power is 0 and electric motor power is 0, a divide by zero error occurs as total system power is equal to 0.	$IHF = 1$, *by definition.*
2. ICE RPM = 0	When ICE is off, IHF = -1 or 1, by definition. This calculation determines the IHF sign based on the direction of electric motor power (i.e., regenerative braking or deceleration vs. electric only acceleration). The absolute value of the denominator allows for the numerator to identify if IHF is negative or positive. Otherwise, there would be no distinction between regenerative operation versus electric drive only operation.	$IHF = \frac{P_{MG2}}{\lvert Total\ System\ Power \rvert} = \frac{Electric\ Motor\ (kW)}{\lvert Electric\ Motor\ (kW) \rvert}$
3. Electric Motor Power < 0 & Battery Power < 0	If both the electric motor power and battery power are negative, the vehicle is generating power and storing it in the battery. Battery power is therefore the sum of MG1 and MG2.	$IHF = \frac{P_{BAT}}{Total\ System\ Power} = \frac{Battery\ Power\ (kW)}{\lvert 0.72 * ICE\ Power\ (kW) \rvert + \lvert Battery\ Power\ (kW) \rvert}$

Condition #	Description / Rationale	Resulting IHF Expression
4. Electric Motor Power >= 0 & Battery Power <= 0	When the electric motor is positive and the battery is negative, MG1 is generating more power than MG2 can use; that power is stored in the battery	$IHF = \frac{P_{MG2+}P_{BAT}}{Total\ System\ Power} = \frac{Electric\ Motor\ (kW) + \lvert Battery\ Power\ (kW)\rvert}{\lvert 0.72 * ICE\ Power\ (kW)\rvert + Electric\ Motor\ (kW) + \lvert Battery\ Power\ (kW)\rvert}$
5. Electric Motor Power >=0 & Battery Power >= 0	When the electric motor is positive and the battery is positive, the battery is supplying additional power to MG2 that MG1 cannot supply. This means the battery power is accounted for in the electric motor (MG2) power output	$IHF = \frac{P_{MG2+}P_{BAT}}{Total\ System\ Power} = \frac{Electric\ Motor\ (kW)}{\lvert 0.72 * ICE\ Power\ (kW)\rvert + Electric\ Motor\ (kW)}$
6. Electric Motor Power < 0 & Battery Power > 0	At higher vehicle speeds, MG1 may act as a motor while MG2 acts as a generator. This occurs under coasting/light pedal usage. Toyota describes MG1 as controlling the ECVT in the mode. It's unclear if this power makes its way to drive the wheels or is just used for transmission control	$IHF = \frac{P_{MG2+}P_{BAT}}{Total\ System\ Power} = \frac{Electric\ Motor\ (kW) + \lvert Battery\ Power\ (kW)\rvert}{\lvert 0.72 * ICE\ Power\ (kW)\rvert + \lvert Electric\ Motor\ (kW)\rvert + BatteryPower\ (kW)}$

* IF/THEN statements are evaluated in order of conditions 1 to 6. The factor 0.72 in the IHF equation represents the fixed proportion of ICE power used to drive the wheels determined from the planetary gearset gear teeth ratios.

Table 3. IHF Value Interpretation Summary and Relationship to Conditional Statements

IHF Value	Interpretation	Conditions
-1	ICE off, vehicle is moving but coasting, creating regenerative power	2
-0.99 to -0.01	Power is net regenerative. ICE on, vehicle may or may not be stationary, regenerative braking and/or MG1 power generation.	3, 6
0	Rare condition in dataset (225 points not flagged under restart), ICE on, vehicle stationary or "creeping".	4, 5
0.01 to 0.99	ICE on, MG1 power used by MG2 for moving vehicle, battery may/may not be adding power depending on MG2 demand, excess MG1 power sent to battery.	4, 5, 6
1	ICE off, vehicle stationary or moving under MG2 power (from battery) only	1, 2

NOTE: Recirculation was observed under low vehicle power demand when the vehicle was coasting or decelerating at vehicle speeds above the 42 mph ICE-off threshold. Recirculation results in IHF = -0.99 to -0.01.

The first term in the denominator of Equation 7 represents the fixed fraction (72%) of ICE torque available to drive wheels, as reported in the literature. For a significant portion of the data, additional power was being generated by the generator, but it was not being directly used by the electric motor to drive the wheels. This was due to the mechanical link between the ICE and the MG1 generator. IHF accounts for this additional power in the Equation 7 denominator (Total System Power). We determined that accounting for excess energy storage in the IHF calculation was critical, because energy storage has a determining effect on vehicle operation and subsequent emissions. In other words, power stored at time t may be used to reduce the need for combustion-related power at later times, greater than t+1.

Electric Motor/Generator 2 (MG2) and Vehicle Speed

Negoro and Purwadi (2013) concluded that the Toyota Camry operates with MG2 as the main propulsion device [32]. This is likely true under low vehicle speed operation when the electric motor contributes a significant portion of torque to the wheels (city driving). During high vehicle speed operation, the ICE is the main propulsion device. This is consistent with mileage ratings because the relative CV vs. HEV fuel economy ratings are significantly different during city driving (22 mpg vs. 33 mpg), but quite similar for highway (32 mpg vs. 34 mpg). Considerable IHF development effort involved examination of the raw scantool data for MG1 and MG2 speed (RPM) and torque to properly assign values to P_{MG2} and $P_{Battery}$ in Equation 7. Because of the way the scantool recorded data, negative battery power indicated excess power being stored to the battery.

Because MG2 is mechanically linked to the wheels, as long as the vehicle is driving forward, MG2's RPM is always positive. So, if MG2 torque is positive, MG2 power is positive and therefore MG2 is acting as a motor. If MG2 torque is negative, MG2 is acting as a generator,

meaning the vehicle is coasting/decelerating/braking. MG1 behavior is more complicated than MG2 because MG1 is mechanically linked to the ICE, therefore MG1's RPM and torque could be positive or negative. In the development of IHF, MG1's behavior was thoroughly analyzed to be able to determine the direction of power flow for computing battery power. The ICE is mechanically linked to the sun gear 1 (MG1) and the electric motor (MG2) is mechanically linked to the sun gear 2, but the ICE has no mechanical link to the electric motor, meaning the electric motor can operate freely on its own. The rotation rate of MG2 is equal to the rotation rate of the wheels, and therefore directly related to vehicle speed, as demonstrated in Figure 4. This confirms the observation by Negoro and Purwadi (2013) that MG2 is the primary drive motor and the ICE assists in propulsion. The ICE will never drive the wheels independently. During regenerative braking, MG2 continues to rotate with the wheels, but the electric field is reversed, changing the direction of the torque and generating electrical power.

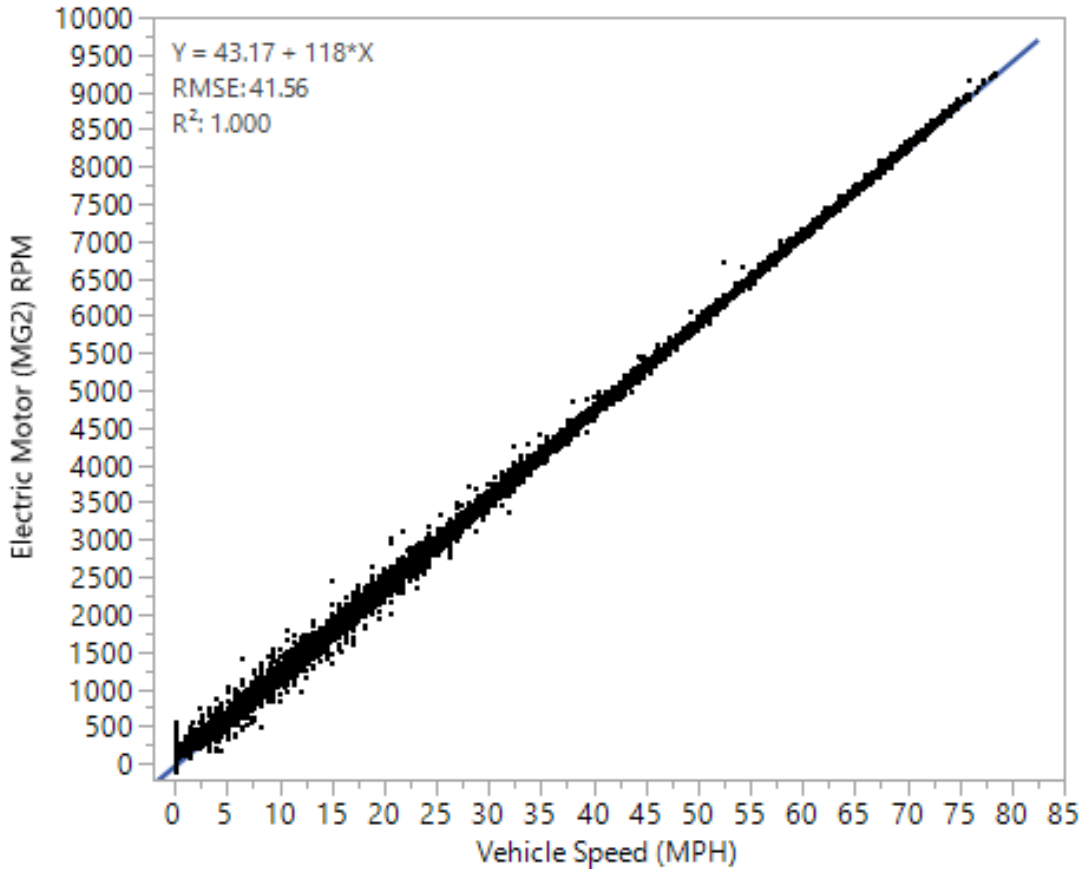

Figure 4. Relationship between the electric motor speed (RPM of MG2) and the vehicle speed (MPH) due to the mechanical link between the electric motor MG2 and the wheels.

Related to the design of the 2010 Toyota Camry HEV is the observation that the ICE was not able to turn off above vehicle speeds of approximately 42 mph. The maximum speed recorded in the dataset for ICE-off operation was 40.4 mph before restart. This observation is also explained by the mechanical linkage between the ICE and MG1. When the ICE is off, MG1 spins freely (T_{MG1} = 0 Nm), but at higher vehicle speeds (above the threshold speed of ~42 mph for

this vehicle), control of MG1's rotation rate is apparently achieved by restarting the ICE so it can apply torque to MG1 to slow its rotation rate. We would expect differences in the pattern of battery recharge/discharge rates above and below this vehicle speed threshold, and these were observed (Figure 5). In Figure 5, the HEV's high voltage battery energy (Wh/s) is plotted by VSP bin, with blue symbols indicating negative VSP and red symbols positive VSP. Both speed classes showed similar net recharge rates of the HVB when Battery Energy was negative, chiefly occurring during negative VSP operation. However, for positive VSP operation, higher net discharge of the HVB occurred during lower-speed driving, likely due to more overall reliance on battery propulsion in stop-and-go driving conditions, although we did not examine by road type. Further, the VSP cross-over from net recharge to net discharge (x-intercept at y=0) was about 7 kW/ton for low speed driving and increased to 15 kW/ton for speeds > 42mph (Figure 5). The lower cross-over VSP for driving at speeds typical of CBD (25 MPH speed limit) and Suburban Arterial driving (40 MPH posted speed limit), reflects more high voltage battery (HVB) involvement in propulsion under these driving conditions. Apparently at higher speeds, the HEV systems are continuously regenerating the HVB, most likely during feathering of the accelerator pedal during near-steady higher speed operation.

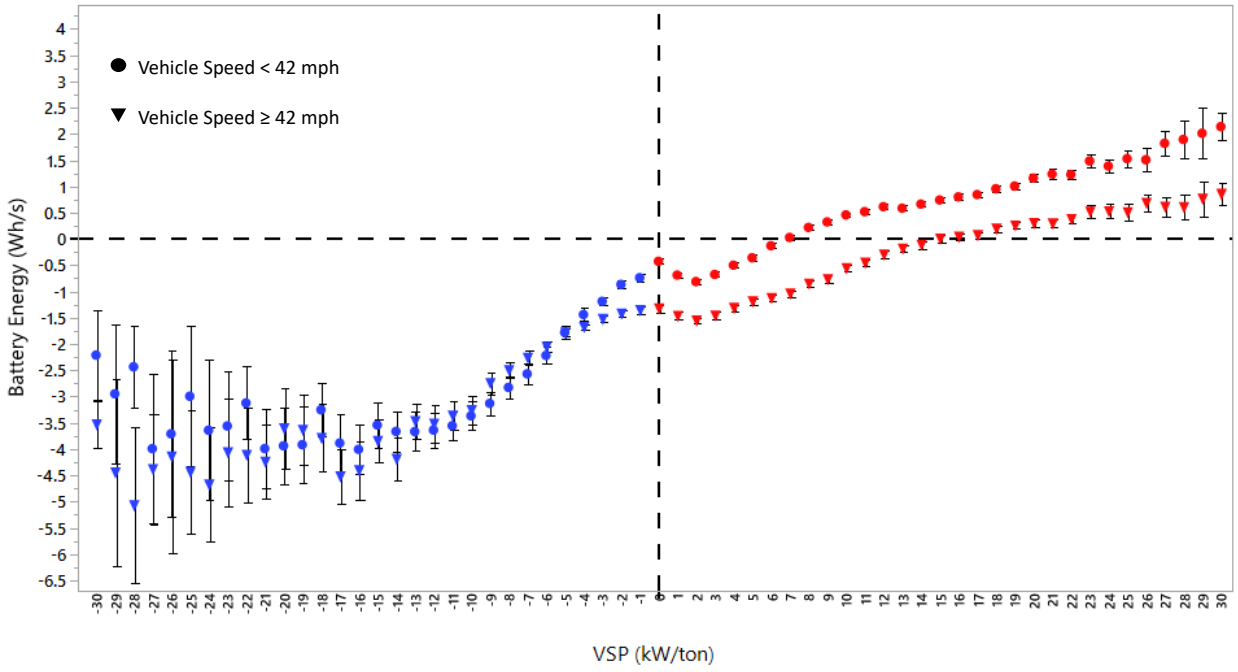

Figure 5. High voltage battery (HVB) energy for two vehicle speed classes. The HEV's ICE could only shut down when vehicle speed was < 42 mph (shown as circles). Net battery discharge is indicated by positive values of Battery Energy and net recharge by negative values.

Figure 6 compares the HVB's recharge/discharge rates for driving with the ICE ON vs. OFF, showing distinct differences in VSP range of coverage as well as overall pattern.

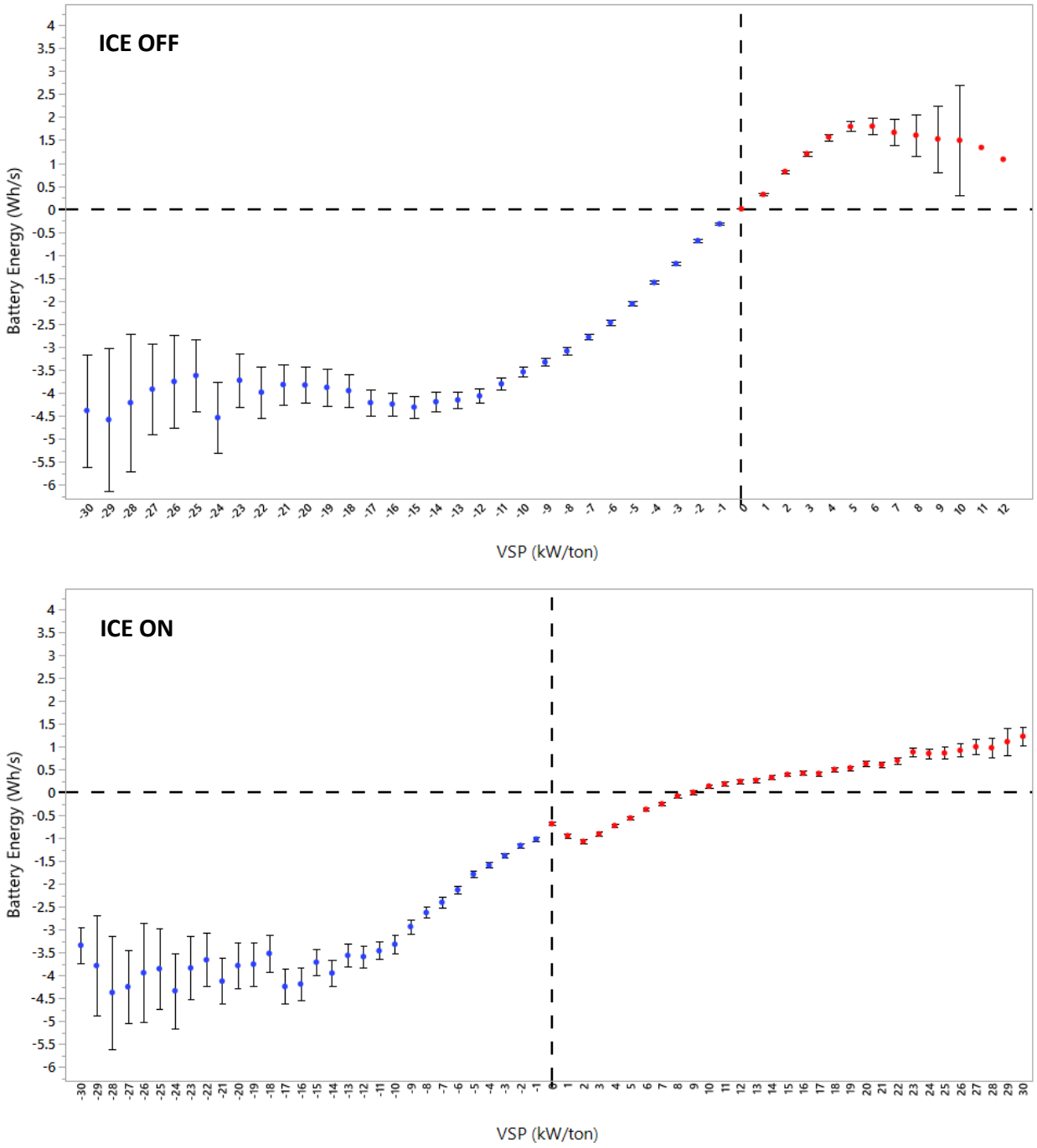

Figure 6. Computed HV Battery rate of discharge (positive values of Wh/s) and recharge (negative values of Wh/s) as a function of VSP for data when the HEV's ICE was off (top) and on (bottom). Note the differences in the x-axis scale between the two plots. The vertical and horizontal dashed lines denote values of zero.

HEV Operating States

Ten different operating states of the HEV were recognized based on scantool sign conventions used to quantify IHF, but these were broadly categorized into 3 fundamental operating states, as follows (referencing power flows in Figure 3).

1. **Electric drive only (EDO) operation** occurred only when the **ICE was off** (ICE RPM = 0). The vehicle was either stopped or in motion, but all power was provided by the electric system. This state results in an IHF of either -1 or +1, where -1 represents regeneration with the ICE off (Figure 3, dashed red line) and +1 represents 100% electric drive propulsion with the ICE off (see Figure 3, solid red line). MG1 spins freely during EDO operation (i.e., MG1 torque = 0).
2. **Power recovery** occurs during **ICE-on** operation with MG2 acting as a generator. MG2 is mechanically connected to the wheels, so the MG2 rotation rate is always positive (unless driving in reverse) and proportional to vehicle speed. During periods of deceleration (coasting or braking), MG2 torque is negative, producing negative power, or power generation that is stored in the 30 kW high voltage battery (Figure 3, blue dashed line). Electric power generated by MG1 via the ICE is also used to charge the high voltage battery (Figure 3, dashed blue line). During moderate to high speed operation when the ICE could not turn off (e.g., vehicle speed > 42 mph for the study HEV), power created by MG2 may be recirculated to MG1 instead of being utilized as regenerative battery power (Figure 3, blue dotted line). MG1 is then operated as a motor instead of a generator to control the power split device (PSD). Recirculation was observed under low vehicle power demand when the vehicle was coasting or decelerating at vehicle speeds above the 42 mph ICE-off threshold. The combined regeneration/recirculation with ICE-on HEV operating state resulted in negative IHF values between -0.01 and -0.99.
3. **Electric drive assist** also occurred during **ICE-on** operation, but with MG2 acting as a motor. During electric drive assist operation, the ICE powers both the wheels and MG1. MG1 generates electrical power that is used to power MG2, which then powers the wheels (Figure 3, green solid line). Excess power generation by MG1 is used to charge the 30 kW high voltage battery (Figure 3, green dashed line). During periods of high power demand, where the 40 kW MG1 maximum power cannot supply the power demand of MG2, the high voltage battery can contribute additional power up to 30 kW (Figure 3, green dotted line). During drive assist operation, positive IHF values ranged between 0.01 and 0.99, with higher values indicating more electric motor contribution to overall propulsion.

The complexity of the planetary combination gearing means that the ICE and electric motors do not operate independently in this vehicle system. As shown below, as vehicle load increases (as quantified by VSP), IHF trends towards 0.5 to 0.6, meaning about 50% of the total power generated in one second is provided by the electric system, at full load. Further, drive power goes through the electric motor regardless of whether that power comes from the ICE (via the

generator, MG1) or from the HV battery. The battery provides relatively little power for the vehicle except during higher load demands.

Instantaneous Hybridization Factor and Road Type and Vehicle Speed

To examine the power-split distribution across the full TOTEMS dataset, IHF was classified into 13 separate bins and the frequency of operation in each bin, by road type was tabulated (Table 4). The "Restart" column in Table 4 represents the 4,660 data record subset for ICE-restart events at the first recorded second of ICE RPM > 0 following ICE-off.

In the extremes, when the vehicle was stationary with the ICE off, IHF = +1 (Bin 13) and IHF = -1 (Bin 1) occurred when the vehicle was in motion and MG2 acted as a generator to recharge the HVB. IHF bin 7 was a rare event in the data, accounting for 151 total records over all road types and occurred during just 2 runs; 46 events in run 17 and 61 events in run 47 during CBD driving. No reason was identified to distinguish these 2 runs.

In total, 37% of the data was under ICE-off operation (IHF bins 1 and 13 combined). Higher ICE load conditions measured from the scantool (load > 80%) on CBD, rural and suburban arterial driving resulted in IHF trending towards bin 9 (29%) and bin 10 (53%). High load on the freeway saw IHF primarily in bins 8 (16%) and 9 (70%). During the relatively lower speed CBD and suburban arterial driving, 51% and 52% of the data resulted in ICE-off operation, with 35% and 27% in bins 9-12, respectively. This indicates a high portion of power assist from the electric motor during urban driving in response to traffic signals and congestion. Just 13% of CBD and 20% of suburban arterial driving was regeneration/recirculation (IHF bins 2-6). In contrast, IHF during freeway driving primarily falls between bin 2 and bin 9 (with 60% in bins 2-6, for comparison), indicating regeneration or recirculation as the primary operating state and less power assist from the electric motor. Only 5% of data on the freeway falls in bins 10 to 12. Because the ICE does not turn off at freeway speeds, EDO may only occur on the on-ramp/off-ramp. Rural driving encompasses a wider range of IHF states; 28% ICE-off, 37% in IHF modes 9-12 and 35% in IHF bins 2-6. ICE-off operation during rural driving occurred during deceleration and coasting at speeds below the 42 mph ICE-off threshold, or at controlled intersections. Further, 60% of all EDO drive operation (IHF = +1) was during idle operation when vehicle speed = 0 mph.

Table 4. Percent of TOTEMS driving data within each IHF bin, by road type and for restart events*

IHF Bin	HEV Driving Condition	IHF Value	Road Type (Defined by Speed Limit)				% All Data	Restart
			CBD (25 mph)	Suburban Arterial (40 mph)	Rural (45 mph)	Freeway (65 mph)		
1	EDO: Regen	-1	24%	27%	17%	3%	19%	0%
2	ICE-on: regeneration or power recirculation	-0.99 to -0.81	5%	3%	10%	12%	7%	2%
3		-0.80 to -0.61	3%	3%	6%	9%	4%	1%
4		-0.60 to -0.41	4%	9%	11%	12%	8%	4%
5		-0.40 to -0.21	1%	4%	6%	17%	6%	2%
6		-0.20 to -0.01	0.4%	1%	2%	10%	2%	0.3%
7	No MG2 assist	0	0.26%	0.01%	0%	0.02%	0.1%	0%
8	ICE-on: MG2 Drive Assist	0.01 to 0.20	1%	1%	2%	10%	3%	1%
9		0.21 to 0.40	4%	7%	12%	22%	10%	7%
10		0.41 to 0.60	20%	13%	18%	3%	15%	24%
11		0.61 to 0.80	7%	2%	3%	1%	4%	32%
12		0.81 to 0.99	4%	5%	4%	1%	4%	26%
13	EDO: Drive	1	27%	25%	11%	1%	18%	0%

*To visually associate IHF bins with HEV driving operations, the Road Type section is conditionally formatted across all road types whereas the All Data and Restart columns are each conditionally formatted separately

Figure 7 shows the mean IHF by speed bins, clearly documenting that higher vehicle speeds are associated with negative values of IHF, in agreement with the data in Table 4. This indicates battery power was used to maintain higher speeds. Recall, it was determined that for the 2010 Toyota Camry, a speed threshold existed at ~42 mph above which the ICE did not shut down. The HEV's battery energy profiles as a function of VSP were different for speeds above and below 42 mph (see Figure 5).

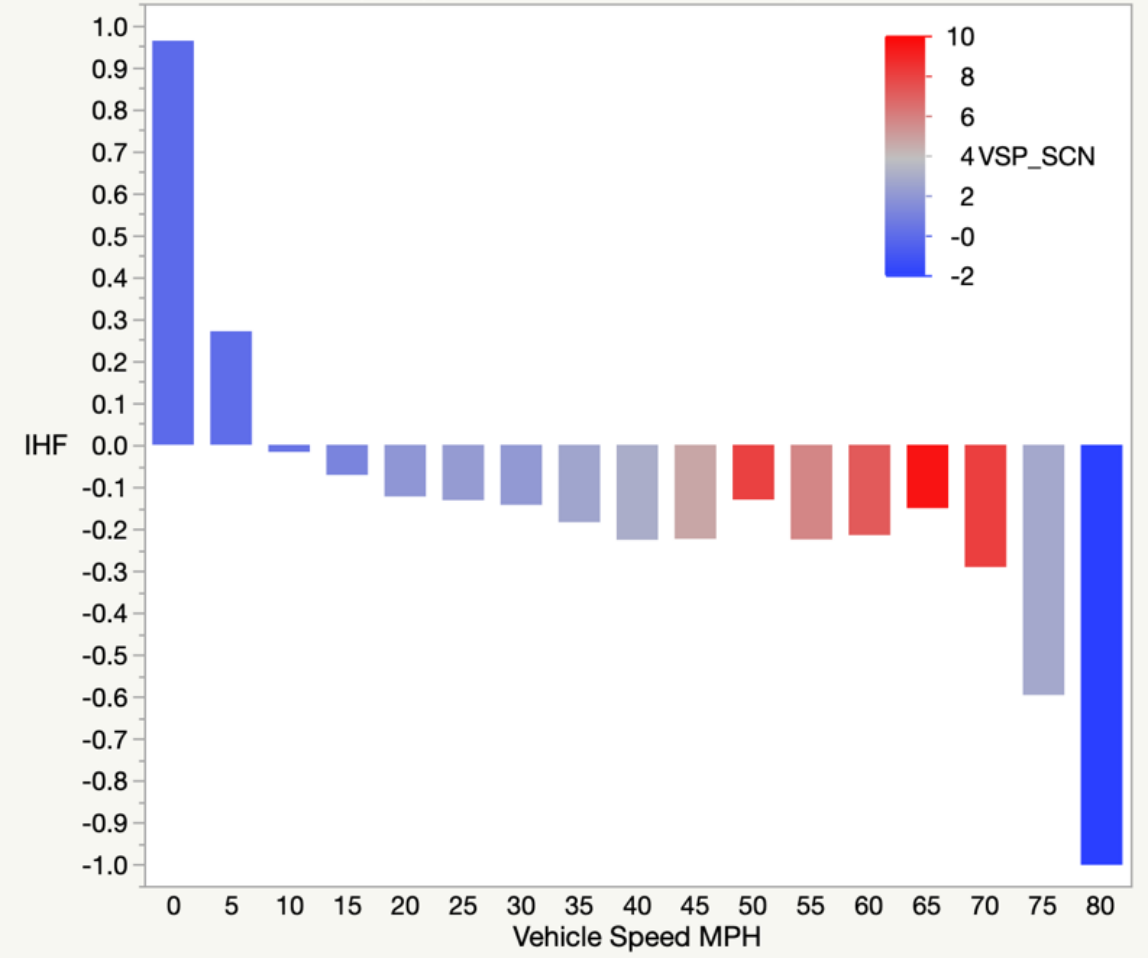

Figure 7. Mean IHF by 5 mph vehicle speed bins. Color of bars represent average VSP for range shown in legend.

Instantaneous Hybridization Factor and VSP

A boxplot of IHF vs. VSP (Figure 8) shows an S-shaped curve of the IHF mean values with lower values at (-) VSP of about -0.95, a rapid increase between VSP = -5 to +2 kW/ton, and upper IHF values (~0.4) stabilized at VSP > 20 kW/ton. Considering all data where VSP < 0 kW/ton, IHF was negative 90% of the time. Figure 8 also shows that electrical regeneration operation (IHF = -1) did not occur at VSP greater than 8 kW/ton, and EDO propulsion (IHF = +1) did not occur at VSP higher than 12 kW/ton. The narrowing of the IHF boxes with increasing VSP should be noted as representing the more limited range of HEV operating states under high load (VSP) driving conditions. Here, narrowing began to occur at VSP ~ 9 kW/ton. Thus, only between VSP = -1 to 8 kW/ton were both EDO regen and EDO drive possible for this HEV.

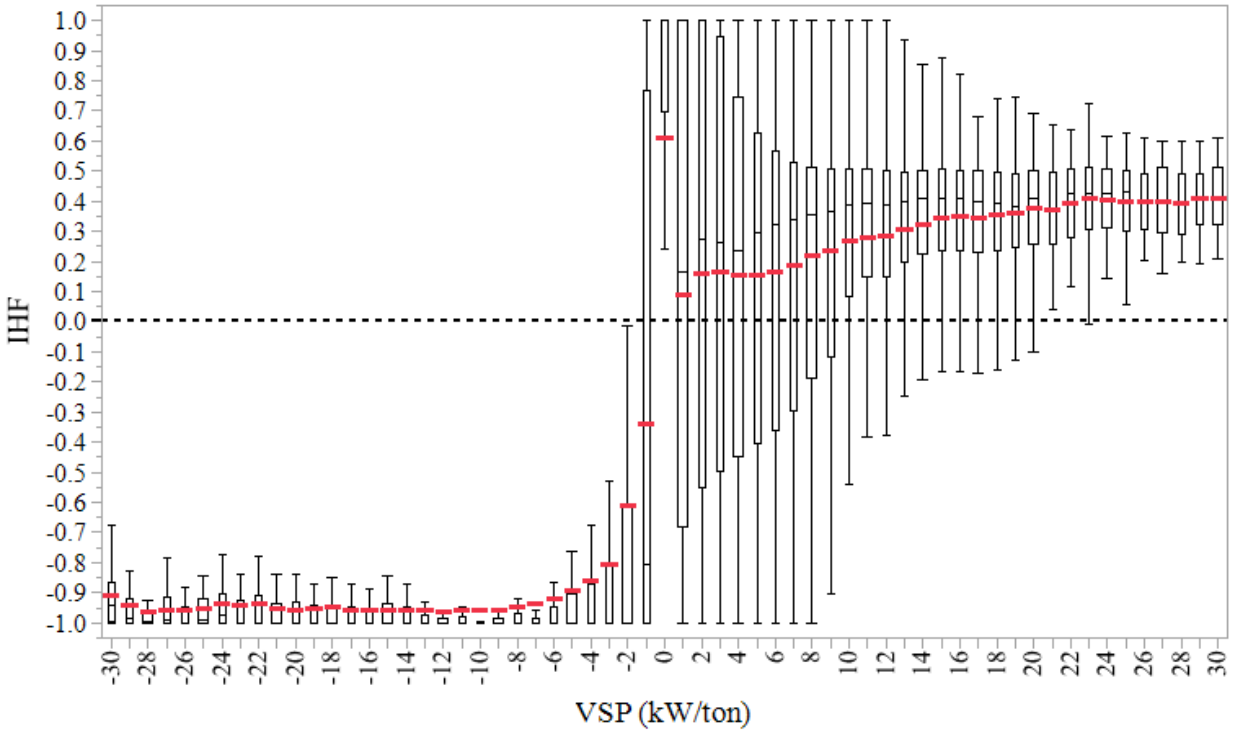

Figure 8. Boxplots of IHF for VSP rounded to the nearest 1 kW/ton integer. Red lines represent the mean IHF. The horizontal dotted line represents IHF = 0.

As calculated load increases, IHF trends towards 0.5 to 0.6 during lower vehicle speed operation (i.e., CBD) and 0.3 to 0.4 for high vehicle speed operation (i.e., freeway). These IHF ranges represent the regions of highest fuel use and subsequently CO_2 emissions. Figure 8 includes data for the entire run. When data were sub-divided into two speed classes, above and below the speed threshold for ICE shutdown, 42 mph, the box plots change considerably (data not shown, see Robinson & Holmén, 2020). There was higher variability in IHF at the highest VSP only for speeds > 42 mph, whereas low speed HEV operation showed consistent IHF values of 0.5 to 0.6.

Given the relationship of IHF to VSP, and knowledge that vehicle emissions are negligible for negative VSP, it is possible that IHF can be used in conjunction with VSP, both being computed based on OBD data, to develop models for HEV tailpipe emissions. This was investigated preliminarily with linear models for CO_2 and PN emission rates, with resulting good model prediction for CO_2, but very poor fits for PN (see Robinson & Holmén, 2020). Possible reasons for the inability of IHF to improve VSP models for HEV emission of PN include the fact that restart events generate extremely high PN emission rates that cannot be captured by the model. Further work is necessary to examine the relationship between IHF just for restart events, a topic not examined in detail in this study.

Conclusions

This research focused on defining the HEV power split calculations for one HEV system based on real-world data. The developed parameter, IHF, an instantaneous (1 Hz) HEV power use metric, may be useful to characterize HEV emissions in terms of the relative electric motor/ICE power contributions. Although this study was limited to one HEV, Toyota's HSD represents the most common HEV system currently on the road and the IHF operating states can be similarly defined for other "full" hybrid passenger cars.

Ultimately the IHF framework may be used to inform differences in HEV vs. CV running emissions based on quantitative understanding of how IHF varies with VSP and vehicle speed, the two vehicle activity variables used to define MOVES operating modes. During vehicle operation when VSP < 0 kW/ton, IHF was negative 90% of the time and frequently resulted in EDO operation when speed was below the 42 mph ICE-off threshold. Therefore, one can assume zero emissions from HEVs for the majority of negative VSP operation. This is an important distinction vs. CVs where low but measurable exhaust emissions occur during deceleration and downhill driving.

VSP of 0 kW/ton resulted in EDO during 80% of total operation, indicating that future research is needed to identify the driving conditions when ICE is on vs. off under zero road load. It is possible that battery state of charge (SOC) may prevent ICE-off operation under cold driving conditions, but the SOC data collected here was too coarse for detailed analysis. For the Toyota Camry HEV studied here, in total, 97% of the VSP = 0 kW/ton operation occurred below the ICE off threshold of 42 mph and 69% of VSP = 0 kW/ton was during idle operation. For the non-idling VSP = 0 condition, negative values of average acceleration (-0.21 mph/s) and road grade (-0.73%) indicate cruise or deceleration on mild road grade was typical. **Therefore, as a first step toward HEV emissions estimation from CV datasets, IHF could be used to identify CV operating data that would translate to zero or near-zero emissions thresholds for HEV vehicles.**

Above VSP = 3 kW/ton, EDO dropped to 23% of total operation, representing a critical VSP range in which the HEV's ICE is being restarted by MG1 and being assisted by the electric motor. ICE restarts (typical IHF = 0.7 to 0.99) at low to moderate vehicle speed are important to identify, as they have previously been shown to result in increased gas-phase and PN emissions [2], [7], [8], [10]. EDO regenerative operation did not occur when VSP > 8 kW/ton (0.05% of all operation at 8 kW/ton). This represents an important distinction for IHF. The range of possible IHF decreased and converged to a mean value of 0.5 to 0.6 under low speed driving conditions typical in urban environments, and 0.3 to 0.4 under high speed driving conditions typical of freeway driving as VSP increased beyond 8 kW/ton. The convergence to relatively narrow points of operation represents the region of highest load on the ICE and the greatest fuel use. EDO drive (IHF = +1) did not occur beyond VSP = 12 kW/ton (0.03% of all operation at 12 kW/ton), meaning the ICE never turned off above VSP = 12 kW/ton, regardless of vehicle speed.

HEV sales projections indicate HEVs will continue to grow as part of the passenger fleet. Past studies have indicated important differences in HEV emissions compared to CVs. These

differences are typically correlated with electric assist, EDO operation and ICE restarts. As HEVs, and new technologies such as single integrated starter-generators ("stop-start" vehicles) continue to make up a greater proportion of on-road vehicles, it becomes increasingly important to account for these technologies in emissions models. Of great importance to human exposure and health in urban areas is in-depth analysis of the restart PN emissions with higher temporal resolution PEMS data collection. IHF may have the ability to take the special operating states of HEVs into account via use of IHF as an adjustment factor (either on the applicable VSP bin, or to directly adjust CV emission rates) to estimate HEV emissions utilizing current CV emissions datasets. More real-world measurements need to be conducted on a wider range of HEVs to evaluate their emissions and operation state behavior under varied driving conditions and to quantify how HEV operation state frequency may change with HEV age.

References

[1] M. K. Robinson and B. A. Holmén, “Hybrid-electric passenger car energy utilization and emissions: Relationships for real-world driving conditions that account for road grade,” *Sci. Total Environ.*, vol. 738, p. 139692, Oct. 2020, doi: 10.1016/j.scitotenv.2020.139692.

[2] M. K. Robinson and B. A. Holmén, “Onboard, Real-World Second-by-Second Particle Number Emissions from 2010 Hybrid and Comparable Conventional Vehicles,” *Transp. Res. Rec.*, vol. 2233, no. 1, pp. 63–71, Jan. 2011, doi: 10.3141/2233-08.

[3] M. Conger and B. A. Holmén, “Characterization of Real-World Particle Number Emissions during Reignition Events from a 2010 Light-Duty Hybrid Electric Vehicle,” *Transp. Res. Rec.*, vol. 2503, no. 1, pp. 137–146, Jan. 2015, doi: 10.3141/2503-15.

[4] US Department of Energy, “U.S. HEV Sales by Model,” *Alternative Fuels Data Center*, 2019. https://afdc.energy.gov/data/10301 (accessed Jun. 17, 2019).

[5] N. Tajitsu, “Toyota to give royalty-free access to hybrid-vehicle patents,” *Reuters*, Apr. 02, 2019.

[6] United States. Department Of Transportation. Bureau Of Transportation Statistics, “Hybrid-Electric, Plug-in Hybrid-Electric and Electric Vehicle Sales,” 2020. https://rosap.ntl.bts.gov/gsearch?collection=dot:35533&type1=mods.title&fedora_terms1=National+Transportation+Statistics (accessed Aug. 07, 2020).

[7] B. A. Holmén and K. M. Sentoff, “Hybrid-Electric Passenger Car Carbon Dioxide and Fuel Consumption Benefits Based on Real-World Driving,” *Environ. Sci. Technol.*, vol. 49, no. 16, pp. 10199–10208, Aug. 2015, doi: 10.1021/acs.est.5b01203.

[8] Y. Huang, N. Surawski, B. Organ, J. Zhou, O. H.H. Tang, and E. Chan, “Fuel consumption and emission performance under real driving: Comparison between hybrid and conventional vehicles,” *Sci. Total Environ.*, vol. 659, pp. 275–282, Dec. 2018.

[9] G. Fontaras, P. Pistikopoulos, and Z. Samaras, “Experimental evaluation of hybrid vehicle fuel economy and pollutant emissions over real-world simulation driving cycles,” *Atmos. Environ.*, vol. 42, no. 18, pp. 4023–4035, Jun. 2008, doi: 10.1016/j.atmosenv.2008.01.053.

[10] M. Christenson, D. Karman, and L. A. Graham, “The Effect of Driving Conditions and Ambient Temperature on Light Duty Gasoline-Electric Hybrid Vehicles (1): Particulate Matter Emission Rates and Size Distributions,” *SAE Trans.*, vol. 116, pp. 1123–1142, 2007.

[11] M. Christenson, A. Loiselle, D. Karman, and L. A. Graham, “The Effect of Driving Conditions and Ambient Temperature on Light Duty Gasoline-Electric Hybrid Vehicles (2): Fuel Consumption and Gaseous Pollutant Emission Rates,” SAE International, Warrendale, PA, SAE Technical Paper 2007-01–2137, Sep. 2007. doi: 10.4271/2007-01-2137.

[12] L. Graham, “Chemical characterization of emissions from advanced technology light-duty vehicles,” *Atmos. Environ.*, vol. 39, no. 13, pp. 2385–2398, Apr. 2005, doi: 10.1016/j.atmosenv.2004.10.049.

[13] F. Reyes, M. Grutter, A. Jazcilevich, and R. González-Oropeza, “Tecnical Note: Analysis of non-regulated vehicular emissions by extractive FTIR spectrometry: tests on a hybrid car in Mexico City,” *Atmospheric Chem. Phys.*, vol. 6, no. 12, pp. 5339–5346, Nov. 2006, doi: https://doi.org/10.5194/acp-6-5339-2006.

[14] J. F. Collins, P. Shepherd, T. D. Durbin, J. Lents, J. Norbeck, and M. Barth, “Measurements of In-Use Emissions from Modern Vehicles Using an On-Board Measurement System,” *Environ. Sci. Technol.*, vol. 41, no. 18, pp. 6554–6561, Sep. 2007, doi: 10.1021/es0627850.

[15] M. Barth, J. Collins, G. Scora, N. Davis, and J. Norbeck, “Measuring and Modeling Emissions from Extremely Low Emitting Vehicles,” *Transp. Res. Rec. J. Transp. Res. Board*, vol. 1987, pp. 21–31, 2006.

[16] G. O. Duarte, R. A. Varella, G. A. Gonçalves, and T. L. Farias, “Effect of battery state of charge on fuel use and pollutant emissions of a full hybrid electric light duty vehicle,” *J. Power Sources*, vol. 246, pp. 377–386, Jan. 2014, doi: 10.1016/j.jpowsour.2013.07.103.

[17] WHO, “Review of evidence on health aspects of air pollution–REVIHAAP project: Final technical report,” 2013.

[18] C. A. Pope III *et al.*, “Lung Cancer, Cardiopulmonary Mortality, and Long-term Exposure to Fine Particulate Air Pollution,” *JAMA*, vol. 287, no. 9, pp. 1132–1141, Mar. 2002, doi: 10.1001/jama.287.9.1132.

[19] A. Valavanidis, K. Fiotakik, and T. Vlachogianni, “Airborne Particulate Matter and Human Health: Toxicological Assessment and Importance of Size and Composition of Particles for Oxidative Damage and Carcinogenic Mechanisms,” *J. Environ. Sci. Health Part C*, vol. 26, no. 4, pp. 339–362, Dec. 2008, doi: 10.1080/10590500802494538.

[20] A. VALAVANIDIS, K. FIOTAKIS, and T. VLACHOGIANNI, “Airborne Particulate Matter and Human Health: Toxicological Assessment and Importance of Size and Composition of Particles for Oxidative Damage and Carcinogenic Mechanisms,” *J. Environ. Sci. Health Part C*, vol. 26, no. 4, pp. 339–362, Dec. 2008, doi: 10.1080/10590500802494538.

[21] C. Holder and J. Gover, “Optimizing the Hybridization Factor for a Parallel Hybrid Electric Small Car,” in *2006 IEEE Vehicle Power and Propulsion Conference*, Sep. 2006, pp. 1–5, doi: 10.1109/VPPC.2006.364359.

[22] A. Somà, “Trends and Hybridization Factor for Heavy-Duty Working Vehicles,” in *Hybrid Electric Vehicles*, IntechOpen, 2017, pp. 11–12.

[23] H. Zhai, H. Christopher Frey, and N. M. Rouphail, “Development of a modal emissions model for a hybrid electric vehicle,” *Transp. Res. Part Transp. Environ.*, vol. 16, no. 6, pp. 444–450, Aug. 2011, doi: 10.1016/j.trd.2011.05.001.

[24] J. L. Jiménez-Palacios, “Understanding and quantifying motor vehicle emissions with vehicle specific power and TILDAS remote sensing,” Ph.D., Massachusetts Institute of Technology, Department of Mechanical Engineering, 1999.

[25] J. Koupal *et al.*, “MOVES2004 Energy and Emission Inputs,” EPA Office of Transportation and Air Quality, Technical Report EPA420-P-05–003.

[26] K. Boriboonsomsin and M. Barth, “Impacts of road grade on fuel consumption and carbon dioxide emissions evidenced by use of advanced navigation systems,” *Transp. Res. Rec.*, vol. 2139, no. 1, pp. 21–30, 2009.

[27] K. Zhang and H. C. Frey, “Road grade estimation for on-road vehicle emissions modeling using light detection and ranging data,” *J. Air Waste Manag. Assoc.*, vol. 56, no. 6, pp. 777–788, 2006.

[28] H. C. Frey, K. Zhang, and N. M. Rouphail, “Fuel Use and Emissions Comparisons for Alternative Routes, Time of Day, Road Grade, and Vehicles Based on In-Use Measurements,” *Environ. Sci. Technol.*, vol. 42, no. 7, pp. 2483–2489, Apr. 2008, doi: 10.1021/es702493v.

[29] B. A. Holmén, “Evaluation of Transportation/Air Quality Model Improvements Based on TOTEMS On-road Driving Style and Tailpipe Emissions Data,” The University of Vermont, 14–012, Jun. 2014. [Online]. Available: http://www.uvm.edu/~transctr/research/trc_reports/UVM-TRC-14-012.pdf.

[30] B. A. Holmén, K. M. Sentoff, M. Robinson, and P. Montane, “The University of Vermont TOTEMS Instrumentation Package for Real-World, On-Board Tailpipe Emissions Monitoring of Conventional and Hybrid Light-Duty Vehicles,” Nov. 2009.

[31] T. A. Burress *et al.*, “Evaluation of the 2007 Toyota Camry Hybrid Synergy Drive System,” United States, Apr. 2008. [Online]. Available: https://www.osti.gov/servlets/purl/928684.

[32] A. B. Negoro and A. Purwadi, “Performance Analysis on Power Train Drive System of the 2012 Toyota Camry Hybrid,” *4th Int. Conf. Electr. Eng. Inform. ICEEI 2013*, vol. 11, pp. 1054–1064, Jan. 2013, doi: 10.1016/j.protcy.2013.12.294.

[33] X. Zeng and J. Wang, “Configuration of Planetary Hybrid Power-Split System,” in *Analysis and Design of the Power-Split Device for Hybrid Systems*, X. Zeng and J. Wang, Eds. Singapore: Springer Singapore, 2018, pp. 25–73.

Data Management

Products of Research

On-board emissions and vehicle operating data were collected by the UVM Transportation Air Quality Laboratory during real-world driving of one HEV and one CV, on a 50 km (32 mi) route over a variety of roadways in Chittenden County, Vermont using the custom Total On- board Tailpipe Emissions Measurement System (TOTEMS). Both vehicles were model year 2010 Toyota Camry of similar driving performance, but different engine size, vehicle weight (due to HEV battery pack) and transmission type.

Data Format and Content

The dataset includes records of time-aligned 1Hz data, including emission rates (# or mass per sec) of criteria, air toxics and particle number (PN) and associated engine and hybrid system operating parameters. Detailed lists of the parameters collected and data collection protocols are available in published UVM Transportation Research Center research reports (Holmén et al. 2014). Sampling conditions for a total of 28 CV and 33 HEV sampling runs were conducted over an 18-month period under ambient temperatures ranging between -13 and 35 °C. Road grade on the driving route was measured independently at sub-meter resolution and varied between -13.2 to +11.5%.

Data Access and Sharing

The TOTEMS dataset used in this project is available on the Dryad data repository associated with the Robinson & Holmén (2020) journal paper published in *Science of the Total Environment* (DOI: 10.1016/j.scitotenv.2020.139692). In addition to the cleaned final dataset, a "Data Dictionary" EXCEL file summarizes the contents of the dataset, with units for each parameter.

Reuse and Redistribution

The TOTEMS HEV-IHF dataset is available at the following link and should be cited as:

> Holmén, Britt; Robinson, Mitchell K. (2020), Hybrid-electric passenger car energy utilization and emissions: Relationships for real-world driving conditions that account for road grade, v2, Dryad, Dataset, https://doi.org/10.5061/dryad.2bvq83bnj

APPENDIX: Detail on Toyota Hybrid System Calculations

2010 Toyota Camry HEV Planetary Gearset Configuration

The inter-relationships between components in the 3rd Generation Toyota Hybrid System was determined based on literature search, including original patents. The dual-planetary gearset configuration used in the MY2010 Toyota Camry HEV has two planetary gears (PGs) that share a ring gear (Figure A1) that ultimately transmits power to the drive wheels: the *power split device (PSD)* planetary gearset 1 (**PG1**) and the *motor speed reduction* planetary gearset 2 (**PG2**). Figure A1 is based on the Zeng and Wang (2018) text, *Analysis and Design of the Power-Split Device for Hybrid Systems*.

Functionally, PG1 (*power split*) balances ICE and MG1 output and PG2 (*speed reduction*) reduces MG2 speed (RPM) to increase MG2 torque to the wheels. As indicated by Figure A1, the ICE has no direct connection to MG2, therefore motor MG2 can operate freely on its own for electric-drive only (EDO) propulsion when ICE is off. MG2 transfers power to Ring 2 in fixed ratio due to the fixed Carrier 2. This ratio is based on relative gear dimensions, as discussed below.

MG1, connected to the sun gear on PG1, has three functions: (1) it acts as the starter motor for the ICE; (2) it turns the sun gear; and (3) as a generator, it charges the HEV's high voltage battery. The ICE drives PG1's pinion gears via a clutch damper and therefore Carrier 1 does not rotate unless the ICE is on.

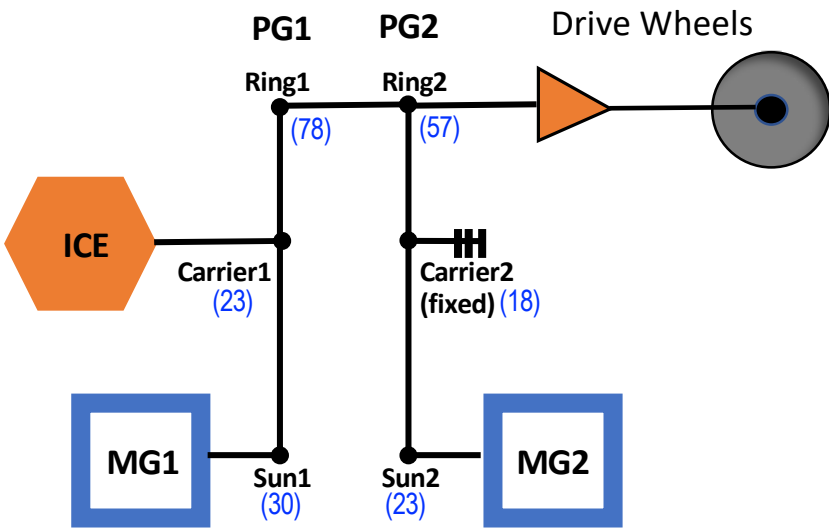

Figure A1. **Configuration of 3rd Generation Toyota Hybrid System components**, after Zeng and Wang (2018), Negoro and Purwadi (2013), Patent CH1819934A and Toyota documentation. Numbers in parentheses are number of gear teeth. Propulsion power from ICE and MG2 is coupled at the shared ring gear (Ring1, Ring2).

Critical to development of IHF using the TOTEMS dataset was the fact that the Toyota Techstream scantool did not allow monitoring of **ICE torque** at the same time the scantool was

reporting HEV controller OBD parameters (see Table 1, main text, for recorded scantool OBD parameters). Thus, available information on the basic operations of planetary gears as well as observations of collected TOTEMS OBD parameter relationships were necessary to compute ICE torque. From ICE torque and recorded ICE engine speed, ICE power, P_{ICE}, was computed from the fundamental relationship, Power = (Torque) * (Engine Speed).

Gear Ratio Determination for Planetary Gearsets

For any meshing type gear, the relative number of gear teeth determines the gear ratio; for planetary gearsets, the gear ratio, i, is:

$$i = \frac{\#\ of\ driven\ gear\ teeth}{\#\ of\ driving\ gear\ teeth} \qquad [A.1]$$

Where "driven" gear is the output and "driving" gear is the input. The PG configuration determines whether ring (R), sun (S) or pinion (planetary gear, P) number of gear teeth, denoted by the letter "z", are used in the gearing ratio calculation. For any planetary gear, t*he sum of the ring and sun gears' number of teeth equals the Planetary Gear teeth, z_P:*

$$z_P = z_R + z_S \qquad [A.2]$$

Also, z_P denotes the planetary carrier behavior because the 'planets' (pinion gears) are attached to the carrier ("planet carrier", C). Depending on the mechanical connections and status of the planetary carrier, three possible cases determine the gear ratio calculation for a single PG based on which of the three components are input, output or stationary (fixed). Equations A.3 to A.6 show example calculations for three planet carrier cases.

(1). ***Carrier as INPUT (Example: R is rotated by C; S is stationary):***

$$i = \frac{z_R}{z_P} = \frac{z_R}{z_R + z_S} \qquad [A.3]$$

(2). ***Carrier as OUTPUT (Example: C is rotated by S; R is stationary):***

$$i = \frac{z_P}{z_S} = \frac{z_R + z_S}{z_S} \qquad [A.4]$$

(3). ***Carrier FIXED (Example: S rotates R):***

$$i = \frac{z_R}{z_S} \qquad [A.5]$$

TOTEMS Dataset ICE/Motor/Generator Behavior Observations.

1. When the ICE was off, MG1 recorded *negative* RPM and zero torque.
2. Torque from MG1 was recorded as *negative* values, with two exceptions:
   (1) when MG1 started the ICE; and
   (2) under EDO (ICE=off), when Carrier 1 does not spin. In this case, MG1 records zero torque, but *negative* RPM.
3. Positive MG1 torque, especially for restart, could often be missing in the TOTEMS dataset because of the sub-second duration of ICE start. MG1 spins the ICE to a certain threshold (reported as 1000 RPM) before spark.
4. MG1 can start ICE in order to charge the HV battery
5. ICE has no connection to MG2 – so MG2 can operate freely on its own.
6. The ICE did not turn off above a threshold vehicle speed – this was interpreted to ICE being used to protect the free-spinning ("overspeed") of sun gear 1 (MG1). The ICE turned on to apply torque to sun gear 1 and slow its RPM to protect MG1. The power generated was stored to the HV battery.
7. During coasting/deceleration at speeds greater than threshold, ICE recorded negative torque, MG1 recorded positive.
8. When vehicle stationary and ICE = ON, Carrier 1 spins to provide torque to sun gear 1 and MG1 generates electrical power that is stored to the HV battery.
9. When both ICE and MG2 operating, ring gear receives torque from both propulsion sources – from Carrier 1 for ICE and directly from MG2 – and electricity generated at MG1 by ICE rotation is sent to MG2 and/or HV battery.

Calculating ICE Torque Contributions.

From the mechanical connections (Figure A1), it can be assumed that the torque contribution from the ICE to both sun gear 1 and ring gear 1 are constant. An important note is **torque contribution** is fixed, but **power output** varies based on ICE engine speed (RPM). The final ring gear total torque includes the contribution from both the ICE and MG2, but our interest here is determining the fraction of torque generated by the ICE that is directed to MG1 (via sun gear 1) versus to the drive wheels via ring gear 1.

Because the ICE has a mechanical link to MG1 (via sung gear 1), the MG1 torque OBD measurement was used to calculate ICE torque, the parameter that could not be simultaneously recorded by the Toyota Techstream scantool. First, the gear information for PG1 and PG2 were obtained from the literature and gear ratios, denoted as K, were computed based on the ratio of the number of teeth in the ring and sun gears of each planetary gearset (Table A1).

Table A1. **Planetary Gear Information** (Negoro and Purwadi, 2013)

Planetary Gear Set 1:	**Planetary Gear set 2:**
Ring = 78 teeth	Ring = 57
Sun = 30 teeth	Sun = 23
K = (78/30) = 2.6	K = (57/23) = 2.478

The interaction between the ICE and MG1 correspond to planetary gear set 1, so torque was computed based on PG1 ring and sun gear teeth, noting Equation A.2 and Table A1 values. The torque output to ring gear 1 (R1) from input by the ICE planetary carrier (PC) is computed to be:

$$T_{R1} = \frac{78}{108} T_{PC} = 0.722\ T_{PC} \qquad [A.6]$$

Similarly, torque output to sun gear 1 (S1) from the ICE used to drive MG1 is:

$$T_{S1} = \frac{30}{108} T_{PC} = 0.277\ T_{PC} \qquad [A.7]$$

Therefore, the constant proportion of torque from the ICE (Carrier 1) to Sun1 (MG1) is approximately 28%, and to Ring1 for drive propulsion is 72%, as denoted in Figure 2 (main text). Rearranging equation A.7 to solve for the torque on the planet carrier (T_{PC}) gives the corresponding equation used to compute ICE torque (in Newton-meters):

$$\mathbf{T_{ICE}(Nm)} = T_{pc} = \frac{T_{MG1}}{0.28} * (-1) \qquad [A.8]$$

Multiplying by (-1) in Equation A.8 corrects the direction of torque based on the observation that recorded torque from MG1 is negative relative to ICE torque in the TOTEMS dataset. Finally, power from the ICE is calculated as the product of torque (T_{ICE}, in Nm) and engine speed (N_{ICE}, in RPM), with constants to convert from units reported by Techstream software (see Table 1, main text):

$$\boldsymbol{P_{ICE}}[kW] = \frac{T_{ICE} * N_{ICE}}{7121} * 0.7457 \qquad [A.9]$$

In summary, approximately 28% of the torque from ICE is used to drive MG1 and the remaining 72% of the ICE's torque is sent to the power-split device to subsequently assist in driving the wheels. The resulting power proportion from ICE to MG1 each second affects the calculation of battery power in the IHF calculation because IHF accounts for total system power generated and stored each second, not drive power output, in the denominator of the stylized IHF equation (Equation 7, main text).

Drive Power Output vs Total System Power

The total output power to the wheels was calculated using the equations *from Zeng and Wang (2018*) as documented in Equations 3 and 4 of the main text (reproduced here).

$$\mathbf{T_{out}(Nm)} = \mathbf{T_{ICE}}\left[\frac{\mathbf{K_1}}{\mathbf{1+K_1}}\right] + \mathbf{T_{MG2}} * \mathbf{K_2} \qquad (3)$$

$$\mathbf{N_{out}(RPM)} = \mathbf{N_{ICE}}\left[\frac{\mathbf{1+K_1}}{\mathbf{K_1}}\right] - \frac{\mathbf{1}}{\mathbf{K_1}}\mathbf{N_{MG1}} \qquad (4)$$

Where:

T_{out} = Total torque out
T_{ICE} = Engine torque
T_{MG2} = MG2 torque
N_{out} = output speed of driveshaft
N_{ICE} = ICE speed
N_{MG1} = MG1 speed
K_1 = planetary gearset 1 ratio = 30/78 = 2.6
K_2 = planetary gearset 2 ratio = 23/57 = 2.478

Equations 3 and 4 are used to compute the power used to move the vehicle (Equation A.9, and Equation 6 in main text), but this calculation **does not account for power generated that is subsequently stored by the hybrid system** such as during regenerative braking and when ICE excess power is sent to MG1 via sun gear 1. The "Total System Power" was calculated to account for energy stored within the hybrid system at any instant; this stored power could contribute to drive propulsion power requirements at future times, so was included in the IHF calculation. Critical to the Total System Power calculation was understanding how the TOTEMS Techstream data recorded for the electric motor/generators, MG1 and MG2, could be used to calculate HV battery power and flow direction. This was necessary because we did not have any direct measurement of current flow to/from the HV battery.

Battery Power Calculations

Initially, the Toyota sign conventions had to be determined to distinguish current flow to or from the HV battery. The relationship between sign on the MG's recorded torque and speed was deciphered to indicate the sign of the MG power term – with the sign indicating the MG was operating either as a motor (positive sign) or a generator (negative sign). It was determined that when recorded torque and speed signs were different, the MG sign was negative (-) or the MG was operating as a generator; when the signs were the same, the MG sign in the battery calculation was positive (+), indicating MG was operating as a motor. These MG and battery calculation sign conventions are summarized in Table A2.

Battery power was calculated as the sum of the computed power for the two MGs (Equation A.10) taking the sign convention into account.

$$P_{BAT} = P_{MG2} + P_{MG1} \qquad [A.10]$$

If the resulting P_{BAT} calculation is negative, excess power is being sent to the HV battery for storage. If P_{BAT} is computed to be a positive value, the battery is discharging to provide additional power to MG2 that MG1 is not able to provide. Therefore, negative battery power was explicitly included in the "Total System Power" calculation, but positive battery power cases do not result in a P_{BAT} term so as to avoid double-counting.

$$Total\ System\ Power = P_{Total} = [\mathbf{0.72} * \mathbf{P_{ICE}}] + |\mathbf{P_{MG2}}| + |\mathbf{P_{Battery}}| \qquad [A.11]$$

It is also important to recognize that only the 72% of ICE power generated is included in the Total System Power calculation (denominator in stylized Equation 7, main text) shown in Equation A.11 and that there are no explicit terms in Total System Power for P_{MG1}. This occurs in order to avoid double-counting power. The 72% must be factored in to account for the proportion of total ICE torque utilized by MG1 to power MG2 to drive the wheels, as described above. MG1 is therefore not explicitly included in the Total System Power calculation because it is already accounted for within the terms for MG2 and HV battery power, depending on HEV operating condition. The various final equations used to compute Total System Power and IHF are outlined in Table 2 of the main text. The 6 conditional statements used to modify stylized Equation 7 are explained and the remaining terms in IHF equation are documented in the table. For example, Condition 5 only has two terms in the denominator, 0.72 P_{ICE} and P_{MG2}, because if P_{BAT} were also included, it would be double-counting the battery power quantity already embedded in the value of P_{MG2} for this condition.

Table A2. Battery Power Calculation from Recorded Sign of MG2 and MG1 Torque and Speed.

MG2	MG1	Battery Calculation	Battery Sign	IHF State
(-)	(-)	MG2 + MG1	(-)	ICE on Regeneration
(+)	(-)	MG2 - |MG1|	(+)	MG2 Drive Assist
(+)	(+)	MG2 + MG1	(+)	Restart or Light-Load Cruise
(-)	(+)	MG2 + MG1	(-)	Shutdown or Moderate to High Speed Cruise/Deceleration
(-)	0	MG2	(-)	EDO: Regeneration
(+)	0	MG2	(+)	EDO: Drive

* Note: MG1 has zero torque when the ICE is off, but spins freely, so RPM > 0.

MG1 = Power to/from moto/generator 1 that is mechanically connected to ICE
MG2 = Power to/from moto/generator 2 that is mechanically connected to wheels
|MG1| = absolute value of MG1 power, a change in sign is needed to avoid double-counting power flow to/from the HVB

Two conditions were required for battery sign (current flow direction).

(1) Negative Battery:

1. IF MG2 < 0 & $P_{BAT} < 0$

$$P_{Total} = (0.72 * P_{ICE}) + P_{BAT}$$

2. IF MG2 >= 0 & $P_{BAT} <= 0$

$$P_{Total} = (0.72 * P_{ICE}) + MG2 + P_{BAT}$$

Negative battery power is always explicitly included in the Total System Power calculation.

(2) Positive Battery:

1. IF MG2 >= 0 & $P_{BAT} > 0$

$$P_{Total} = (0.72 * P_{ICE}) + MG2$$

Positive battery power is already accounted for in the output power of MG2 and is therefore not included explicitly in the Total System Power" calculation.

Appendix References

Documentation for the function of the Toyota Hybrid System (3rd Generation) was found in the following documents:

Toyota Technician Handbook. Module 2- Hybrid Systems. Technical Training. 256 Hybrid General Service. 36pp.

Negoro, A.B. and A. Purwadi (2013) "Performance Analysis on Power Train Drive System of the 2012 Toyota Camry Hybrid," *4th Int. Conf. Electr. Eng. Inform. ICEEI 2013*, vol. 11, pp. 1054–1064, Jan. 2013, doi: 10.1016/j.protcy.2013.12.294

Zeng, X. and J. Wang (2018) "Configuration of Planetary Hybrid Power-Split System," in *Analysis and Design of the Power-Split Device for Hybrid Systems*, X. Zeng and J. Wang, Eds. Singapore: Springer Singapore, 2018, pp. 25–73

Patent CN1819934A (https://patents.google.com/patent/CN1819934A/en)

Lancereal Limited (2020) Planetary Gears: Principles of Operation. https://www.lancereal.com/planetary-gears-principles-of-operation/

Tec-science (2018) Fundamental equation of planetary gears (Willis equation). https://www.tec-science.com/mechanical-power-transmission/planetary-gear/fundamental-equation-of-planetary-gears-willis-equation/